



UNIVERSIDADE ESTADUAL DE CAMPINAS
SISTEMA DE BIBLIOTECAS DA UNICAMP
REPOSITÓRIO DA PRODUÇÃO CIENTÍFICA E INTELLECTUAL DA UNICAMP

Versão do arquivo anexado / Version of attached file:

Versão do Editor / Published Version

Mais informações no site da editora / Further information on publisher's website:

<https://link.springer.com/article/10.1140/epjp/i2014-14206-0>

DOI: 10.1140/epjp/i2014-14206-0

Direitos autorais / Publisher's copyright statement:

©2014 by Springer. All rights reserved.

DIRETORIA DE TRATAMENTO DA INFORMAÇÃO

Cidade Universitária Zeferino Vaz Barão Geraldo

CEP 13083-970 – Campinas SP

Fone: (19) 3521-6493

<http://www.repositorio.unicamp.br>

Efficient finite-time measurements under thermal regimes

Carlos Alexandre Brasil^{1,a}, Leonardo Andreta de Castro², and Reginaldo de Jesus Napolitano²

¹ Instituto de Física “Gleb Wataghin”, Universidade Estadual de Campinas, P.O. Box 6165, 13083-970 Campinas, SP, Brazil

² Instituto de Física de São Carlos, Universidade de São Paulo, P.O. Box 369, 13560-970 São Carlos, SP, Brazil

Received: 31 July 2014

Published online: 1 October 2014 – © Società Italiana di Fisica / Springer-Verlag 2014

Abstract. Contrary to conventional quantum mechanics, which treats measurement as instantaneous, here we explore a model for finite-time measurement. The main two-level system interacts with the measurement apparatus in a Markovian way described by the Lindblad equation, and with an environment, which does not include the measuring apparatus. To analyse the environmental effects on the final density operator, we use the Redfield approach, allowing us to consider a non-Markovian noise. In the present hybrid theory, to trace out the environmental degrees of freedom, we use a previously developed analytic method based on superoperator algebra and Nakajima-Zwanzig superoperators. Here, we analyse two types of system-environment interaction, phase and amplitude damping, which allows us to conclude that, in general, a finite-time quantum measurement performed during a certain period is more efficient than an instantaneous measurement performed at the end of it, because the rate of change of the populations is attenuated by the system-measurement apparatus interaction.

1 Introduction

The measurement problem in quantum mechanics is responsible for most of the controversy surrounding this theory [1, 2]. While in classical physics the observation of an object does not presuppose any changes of its properties, in quantum mechanics this interaction, far from insignificant, causes profound changes on the object under observation. Besides changing the state of the system, the measurement of a given property can influence the value of another (the case of *conjugate observables* such as position and momentum). Another aggravating aspect is the fact that it is not possible to predict with certainty the result of a specific measurement: quantum mechanics rules allow us to know only the several possible results and their respective probabilities —it is an *ensemble theory*, as found by Born [3, 4] and Dirac [5, 6].

To describe a measurement, it is necessary to expand the wave function in terms of the eigenstates of the observable to be measured: the possible results of the measurement will be the respective eigenvalues of the observable, and the corresponding probabilities will be the square moduli of the expansion coefficients. When the measurement is complete, the wave function reduction takes place, and the state of the system is projected onto the eigenstate corresponding to the eigenvalue obtained. All this was synthesized by von Neumann in his pioneer treatise on quantum mechanics [7], where he states the two possible processes of wave function evolution:

- 1) *Reduction*, when a measurement is made.
- 2) *Unitary evolution* according to the Schrödinger equation, between measurements.

In von Neumann’s original work [7], the transmission of information to the measuring apparatus is described by considering two Hilbert spaces which we shall call I , the *principal system* under observation, and II , the *measurement apparatus*. Here, let $\hat{A}^{(I)}$ be the observable of I to be measured, $\{|a_n\rangle\}$ the set of its eigenfunctions with associated eigenvalues a_n , and let $|\phi^{(I)}\rangle$ be the initial state of the system, given as the linear combination

$$|\phi^{(I)}\rangle = \sum_n c_n |a_n\rangle. \quad (1)$$

^a e-mail: carlosbrasil.physics@gmail.com

Obviously, $|\langle a_n | \phi^{(I)} \rangle|^2$ is the probability to find a_n as the possible result of the measurement. Considering that the measurement results for apparatus II are shown on a scale of values, we define an observable $\hat{B}^{(II)}$ that gives us the pointer position of the eigenvalue b_n (referring to the eigenstate $|b_n\rangle$). In this case, there is a direct correlation between a_n and b_n : the result of the measurement of $\hat{B}^{(II)}$ over II will give b_n only if the result of the measurement of $\hat{A}^{(I)}$ over I gives a_n .

Next, let us define the initial state $|\phi^{(I)}\rangle$ of I —unknown in the sense of its being a linear combination of eigenstates of $\hat{A}^{(I)}$ (the goal of the measurement is to determine the state)—and the initial state $|\phi^{(II)}\rangle$ of II , denoted, for simplicity, by $|b_0\rangle$. The initial state of the combined system $I + II$ will then be

$$|\phi^{(I+II)}(0)\rangle = |\phi^{(I)}\rangle \otimes |\phi^{(II)}\rangle, \quad (2)$$

where

$$\begin{cases} |\phi^{(I)}\rangle = \sum_n c_n |a_n\rangle \\ |\phi^{(II)}\rangle = |b_0\rangle \end{cases}. \quad (3)$$

For simplicity, the \otimes symbol will be omitted from now on. The transmission of information from I to II will be made through the *unitary operation*—*i.e.*, by the *process 2* above—associated to the $\hat{H}_{\text{meas}}^{(I+II)}$ Hamiltonian, which acts over the global system $I + II$. If the measurement extends over a time interval τ , the final global state will be

$$|\phi^{(I+II)}(\tau)\rangle = e^{-\frac{i}{\hbar} \hat{H}_{\text{meas}}^{(I+II)} \tau} |\phi^{(I+II)}(0)\rangle. \quad (4)$$

At this point, von Neumann defines the unitary operator

$$\hat{\Delta} \equiv e^{-\frac{i}{\hbar} \hat{H}_{\text{meas}}^{(I+II)} \tau} \quad (5)$$

to simplify his calculations. The question, then, is how to find a form for $\hat{\Delta}$ that fits the established measurement criteria. This is a simple task and the result is

$$\hat{\Delta} \sum_{m,n} x_{mn} |a_m\rangle |b_n\rangle = \sum_{m,n} x_{mn} |a_m\rangle |b_{m+n}\rangle. \quad (6)$$

It can be shown that applying (5) to (2) gives

$$|\phi^{(I+II)}(\tau)\rangle = \hat{\Delta} |\phi^{(I+II)}(0)\rangle = \hat{\Delta} \sum_n c_n |a_n\rangle |b_0\rangle = \sum_n c_n |a_n\rangle |b_n\rangle.$$

The acquisition of information of the state is made by the process 1 above, with the results having associated probabilities $|c_n|^2$ —Born's rule.

In his work, von Neumann did not explicitly consider the time during which the measurement apparatus interacts with the system because the introduction of $\hat{\Delta}$ eliminates the measurement time τ from the calculations. A way to analyze this time period within the conventional structure of quantum mechanics as a statistical theory (and non-causal in von Neumann's point of view [7]) consists of considering the interaction between the system and the measurement apparatus evolving according to the Schrödinger equation or, more generally, the Liouville-von Neumann equation. In such an approach, we still have an equation for the density operator and, consequently, the probabilistic character of quantum mechanics is still present: the populations provide the associated probabilities for the possible results. Here, the problem of the wave function reduction will not be analyzed and/or refuted—there are, indeed, interpretations of quantum mechanics where the reduction phenomenon is treated as non-existent [8–11].

To clarify this treatment, it is convenient to use a framework that resembles the one by Peres [12], who labeled the procedure of acquiring information regarding the physical system as *intervention*. That procedure is divided into two parts: the *measurement*, when the apparatus interacts with the system and acquires the information, and the *reading* (or *output*), when the results of the intervention become known and the reduction of the wave function occurs. In the last step, the probabilistic information is contained in the populations of the density operator.

As mentioned previously, a more realistic description of the measurement apparatus implies the distinction between its microscopic and macroscopic degrees of freedom. To each possible eigenvalue measured, there is one and only one macroscopic value. However, this variable does not describe completely the state of the measurement apparatus, because there are many microscopic states corresponding to the same value of the macroscopic variable. As in the measurement the only important variable is the macroscopic one, we must take the partial trace over the microscopic variables. Under the Markov approximation for the interaction between the system and the measurement apparatus,

this procedure leads to the *Lindblad equation* [13–15], where only the system coordinates appear. This equation for the density operator has a term for *unitary evolutions* (the *Liouvillian*, already known) and a second term, for the *non-unitary evolutions*, named *Lindbladian*. It is exactly the non-unitary term that allows us to introduce the time interval during the interaction between the system and the measurement apparatus [16]. In the quantum-measurement-theory context, its derivation was suggested in [12] and made in a simple manner in [17].

Until now, we have a situation where only two systems are considered: the system on which the measurement is made (which is the object of our interest), and the measurement apparatus. However, in real situations, the perfect isolation of the system is not always possible to achieve and, consequently, the environment perturbations change the final density operator in some way. To treat this situation, we consider that the system interacts with both the environment and the measurement apparatus, the effects of the environment being introduced in the Liouvillian of the Lindblad equation. In this way, with the partial trace over the environmental degrees of freedom, we obtain an equation in the Lindblad form, provided the environment is assumed as Markovian. To calculate the more general trace over the environmental degrees of freedom appearing in the Lindblad equation, we developed a formalism [18] based on the superoperator algebra and the Nakajima-Zwanzig projectors [19, 20].

It should be noted that alternative methods of describing continuous measurements that do not recur to the Lindblad superoperator exist, and include the introduction of an extra term to the Hamiltonian to account for the interaction with the measurement apparatus [21, 22], and the use of a stochastic master equation [23]. This latter description is not incompatible with the one provided by the Lindblad equation [16], which, for this choice of Lindblad operators, is also equivalent to the master equation for continuous position measurements derived by Barchielli *et al.* and Caves *et al.* [24, 25]. Our choice of employing the Lindblad equation as the starting point of our model, however, has proven satisfactory for the solution of the problem of the noisy finite-time measurement, that is, a finite-time measurement that occurs while the system suffers errors caused by an external environment. The investigation of this problem is what constitutes our original contribution to the field.

In previous papers [18, 26, 27], our formalism was applied to a two-state system in contact with an environment via phase-damping interaction, in the case of an Ohmic spectral density. Under some restrictions —both the natural system frequency and the environmental temperature set to zero— chosen to simplify the problem and allow analytical solutions, we verified that [26], when the measurement does not commute with the system-environment interaction, i) the more intense the system-environment interaction, the more marked is the decrease of the population —*i.e.*, the larger is the measurement error— and ii) the more intense the system-measurement apparatus interaction, the less marked is the rate of change of the populations. From ii), we concluded that finite-time measurements can be more efficient than instantaneous ones, when the measurement does not commute with the interaction between the system and the environment, because the nature of the system-apparatus interaction reduces the rate of change of the populations. To estimate the *efficiency of a measurement*, here, we adopt the criterion that an ideal measurement would consist of the instantaneous acquisition of information from the system before its state was altered by the environmental noise. If the populations of the system have been significantly altered by the time the measurement reaches its completion, the probabilities of encountering the apparatus's pointer in either state will be visibly different from the probabilities associated with the initial state of the system measured, thus rendering the process inefficient. Next, analyzing the behavior of the coherences, which decrease with time, we established a criterion for the measurement duration [27].

In the present work, we remove the restrictions and treat the interaction between the system and the environment as either the phase-damping or the amplitude-damping type, aiming at verifying, in a more general form, the influence of the environment on the final reduced density operator. We verify that, in general, the conclusions obtained in the previous works for state protection and system-environmental coupling apply to both interactions (phase and amplitude damping), even in the case of a finite environmental temperature. The addition of system frequency induces an oscillatory behavior on the populations. For the coherences, however, we observe that the introduction of the system frequency causes their moduli to approach, after a certain time interval, a constant asymptotic value, that may or may not be zero. Although we cannot, in this case, obtain a simple expression for the duration of the measurement, we still use the coherences to establish the time at which the system-environment interaction can be interrupted and the reading of the state accomplished—in this case, the time when the coherences assume the constant asymptotic value. Obviously, in more general cases, when the behavior of the system is not simple (the coherences no longer show a monotonic decrease), its physical properties must be considered in the establishment of the measurement time. Here, we do not change the spectral density and do not increase the number of states of the system under measurement—these extensions are left open and can be more safely developed under the light of the knowledge of the results presented here.

The possibility of application of this kind of measurement to improve the quality of the results depends, however, on the practical existence of measurements that can be performed during a finite period of time, in accordance with the model. There is, however, a recent application of our work—see ref. [28]— in the context of Measurement-based Direct quantum Feedback Control (MDFC) [29, 30].

This article is structured as follows: in sect. 2, we recapitulate our description of noisy finite-time measurements, providing the basis for the solutions obtained in sects. 3 and 4, first for the phase-damping case, and then for the

amplitude-damping one. Analyses of the solutions, together with graphs, are presented in sect. 5, conclusions and perspectives are given in sect. 6. An appendix explains how this model of finite-time measurement could be experimentally tested against the more conservative approach that presupposes instantaneous measurements.

To present the results in a more logical and complete fashion, some of the contents of this article have been recapitulated from our previous works. Section 2 briefly explains the method that can be found, with greater details, in [18] and solutions for the Lindblad equation for the x -component measurement without environment found on [26]; sect. 3 shows the z -component solution and the simplified ($T = 0$ and $\omega_0 = 0$) x -component solutions found on [26] for the phase-damping interaction; finally, in sect. 5 we show the formula for the upper limit for the measurement duration found in [27]. All the other results, however, are new.

2 The model of finite-time measurement

In this section, we overview the model of noisy finite-time measurement that was developed and employed in our previous works [26,27]. This model assumes that the system interacts with the measurement apparatus through a Markovian interaction. However, the finite nature of this description allows for other processes to occur before the measurement reaches its end.

In the usual treatment, when measurements are performed over the *principal system* S , it is assumed that S is perfectly isolated from the environment, interacting non-unitarily with the measurement apparatus. However, as we are considering the measurement as a finite-time process that may take a certain period to reach its completion, here we make the assumption that the system is not isolated, but also interacting with an *environment* B . To deal with this situation, we describe the additional interaction between the system and the environment as a unitary evolution, with the Hamiltonian

$$\hat{H} = \hat{H}_B + \hat{H}_{SB} + \hat{H}_S, \quad (7)$$

where \hat{H}_S and \hat{H}_B are the system and the environment Hamiltonians, and \hat{H}_{SB} is the interaction between them.

Therefore, to model the noisy measurement we describe both the measured object and the environment by a total density operator $\hat{\rho}_{SB}$ obeying the *Lindblad equation* [13–15]:

$$\frac{d}{dt}\hat{\rho}_{SB} = -\frac{i}{\hbar}[\hat{H}, \hat{\rho}_{SB}] + \sum_j \left(\hat{L}_j^{(S)} \hat{\rho}_{SB} \hat{L}_j^{(S)\dagger} - \frac{1}{2} \left\{ \hat{L}_j^{(S)\dagger} \hat{L}_j^{(S)}, \hat{\rho}_{SB} \right\} \right). \quad (8)$$

Here, the first term of the right-hand side, $-\frac{i}{\hbar}[\hat{H}, \hat{\rho}_{SB}]$, is the *Liouvillian* and corresponds to *unitary evolutions*, while the second term, $\sum_j (\hat{L}_j^{(S)} \hat{\rho}_{SB} \hat{L}_j^{(S)\dagger} - \frac{1}{2} \{ \hat{L}_j^{(S)\dagger} \hat{L}_j^{(S)}, \hat{\rho}_{SB} \})$, is the *Lindbladian* and corresponds to the *non-unitary evolutions*. The $\hat{L}_j^{(S)}$ operators are the *Lindblads*, which act only on the system S , and can describe *measurement processes* [12,16,17,26] if they are *Hermitian*, or *dissipation processes* [14], if *non-Hermitian*. When the Lindblads are all zero, we recover the Liouville-von Neumann equation, *i.e.*, there is no measurement occurring.

Here, we are only interested in the reduced density operator $\hat{\rho}_S$ of S . In our formalism [18], this is done with the help of the Nakajima-Zwanzig projectors [19,20] that, for the general operator $\hat{X}(t)$ and the initial instant t_0 , act as

$$\hat{P}\hat{X}(t) \equiv \hat{\rho}_B(t_0) \otimes \text{Tr}_B \left\{ \hat{X}(t) \right\}, \quad (9)$$

$$\hat{Q} \equiv 1 - \hat{P}, \quad (10)$$

where we are using superoperator algebra. In the present case, we have defined superoperators referring to the contributions by the system S

$$\hat{S}\hat{X} = -\frac{i}{\hbar}[\hat{H}_S, \hat{X}] + \sum_j \left(\hat{L}_j^{(S)} \hat{X} \hat{L}_j^{(S)\dagger} - \frac{1}{2} \left\{ \hat{L}_j^{(S)\dagger} \hat{L}_j^{(S)}, \hat{X} \right\} \right), \quad (11)$$

the environment B :

$$\hat{B}\hat{X} = -\frac{i}{\hbar}[\hat{H}_B, \hat{X}], \quad (12)$$

and to the interaction between them,

$$\hat{F}\hat{X} = -\frac{i}{\hbar}[\hat{H}_{SB}, \hat{X}]. \quad (13)$$

With these definitions, we obtain the integral equation

$$\frac{d}{dt} [\hat{P}\hat{\alpha}(t)] = \int_0^t dt' [\hat{P}\hat{G}(t)\hat{G}(t')\hat{P}\hat{\alpha}(t)], \tag{14}$$

where we defined the new “interaction-picture” density operator

$$\hat{\alpha}(t) \equiv \exp\left(-\hat{S}t - \hat{B}t\right)\hat{\rho}_{SB}(t) \tag{15}$$

and the superoperator

$$\hat{G}(t) \equiv \exp\left(-\hat{S}t - \hat{B}t\right)\hat{F}\exp\left(\hat{S}t + \hat{B}t\right). \tag{16}$$

One of the advantages of (14), as verified in [18,26], is to make the contributions referring to S and B easily factorized. Both here and in our previous applications [18,26,27], we have considered S a 2-state system and B the environment, with corresponding Hamiltonians

$$\hat{H}_S = \hbar\omega_0\hat{\sigma}_z, \tag{17}$$

$$\hat{H}_B = \hbar\sum_k\omega_k\hat{b}_k^\dagger\hat{b}_k, \tag{18}$$

and the Lindbladian represented by a single Lindblad operator, with the form

$$\hat{L}^{(S)} = \lambda\hat{\sigma}_j, \quad j = x, z, \quad \lambda \in \mathbb{R}, \tag{19}$$

where \hat{b}_k and \hat{b}_k^\dagger are the destruction and creation operators of the environment B , ω_k are the frequencies associated to each environmental mode, ω_0 is the characteristic frequency of the system S , λ is a constant associated with the intensity of the interaction between the system S and the measurement apparatus, and $\hat{\sigma}_j$ are the Pauli matrices:

$$\hat{\sigma}_z = \begin{pmatrix} 1 & 0 \\ 0 & -1 \end{pmatrix}, \quad \hat{\sigma}_x = \begin{pmatrix} 0 & 1 \\ 1 & 0 \end{pmatrix}, \quad \hat{\sigma}_y = \begin{pmatrix} 0 & -i \\ i & 0 \end{pmatrix}. \tag{20}$$

Furthermore, we have adopted an Ohmic spectral density [14] given by

$$J(\omega) = \eta\omega e^{-\omega/\omega_c}, \quad \eta \geq 0, \quad \omega_c > 0. \tag{21}$$

When we analyse the final density operator $\hat{\rho}_S$, we have to write it in terms of the basis of eigenstates of the measurement apparatus responsible for the Lindblad $\hat{L}^{(S)}$. Since we start our calculations using the basis corresponding to the $\hat{\sigma}_z$ eigenstates, $\{|0\rangle, |1\rangle\}$, the $\hat{L}^{(S)} = \lambda\hat{\sigma}_z$ case will not require additional attention. However, in the $\hat{L}^{(S)} = \lambda\hat{\sigma}_x$ case it will be necessary the change to the basis of the $\hat{\sigma}_x$ eigenstates, $\{|+\rangle, |-\rangle\}$, namely,

$$|\pm\rangle = \frac{|0\rangle \pm |1\rangle}{\sqrt{2}}, \tag{22}$$

using the basis transformation matrix

$$\hat{M} = \frac{1}{\sqrt{2}} \begin{pmatrix} 1 & 1 \\ 1 & -1 \end{pmatrix} = \hat{M}^{-1}. \tag{23}$$

We observe that the basis in which the reduced density operator is written will be specified by the superscript (j), as in $\hat{\rho}_S^{(j)}(t)$.

To solve eq. (14), it is often useful to adopt the notation

$$\hat{R}(t) \equiv e^{-\hat{S}t}\hat{\rho}_S(t), \tag{24}$$

so that

$$\hat{P}\hat{\alpha}(t) = \hat{R}(t)\hat{\rho}_B. \tag{25}$$

In the end, the density operator for the system can be recovered simply by applying the inverse transformation

$$\hat{\rho}_S(t) = e^{\hat{S}t}\hat{R}(t). \tag{26}$$

With the definition of $\hat{R}(t)$, the integrand of eq. (14) can be expanded. We illustrate how this is done for the specific case of a phase-damping interaction,

$$\hat{H}_{SB} = \hat{\sigma}_z \sum_k \hbar (g_k b_k^\dagger + g_k^* b_k), \quad (27)$$

where the g_k are the associated coefficients of the spectral density. In this case, $\hat{G}(t)\hat{G}(t')\hat{R}(t)\hat{\rho}_B$ from eq. (16) yields

$$\begin{aligned} \hat{G}(t)\hat{G}(t')\hat{R}(t)\hat{\rho}_B &= ie^{-\hat{S}t}e^{-\hat{B}t}\hat{F} \left\{ e^{\hat{S}(t-t')} \left[\left(e^{\hat{S}t'} \hat{R}(t) \right) \hat{\sigma}_z \right] \right\} \left\{ e^{\hat{B}(t-t')} \left[\left(e^{\hat{B}t'} \hat{\rho}_B \right) \sum_k \hbar (g_k b_k^\dagger + g_k^* b_k) \right] \right\} \\ &- ie^{-\hat{S}t}e^{-\hat{B}t}\hat{F} \left\{ e^{\hat{S}(t-t')} \left[\hat{\sigma}_z \left(e^{\hat{S}t'} \hat{R}(t) \right) \right] \right\} \left\{ e^{\hat{B}(t-t')} \left[\sum_k \hbar (g_k b_k^\dagger + g_k^* b_k) \left(e^{\hat{B}t'} \hat{\rho}_B \right) \right] \right\}. \end{aligned} \quad (28)$$

The following procedure is to replace the superoperators in eq. (28) with the definitions from (11), (12) and (13). To do this, it is necessary to clarify the effect of the temporal exponentials of the superoperators, $e^{\hat{S}t}$ and $e^{\hat{B}t}$. For example, defining \hat{X}' as the result of applying $e^{\hat{B}t}$ on an operator \hat{X} :

$$\hat{X}' = e^{\hat{B}t} \hat{X} \quad (29)$$

and taking the time derivative on both sides, we have

$$\frac{d}{dt} \hat{X}' = \hat{B} e^{\hat{B}t} \hat{X} = \hat{B} \hat{X}', \quad (30)$$

but, by the definition (12), eq. (30) will be

$$\frac{d}{dt} \hat{X}' = -\frac{i}{\hbar} [\hat{H}_B, \hat{X}']. \quad (31)$$

This is the Liouville-von Neumann equation, whose solution, for a time-independent Hamiltonian \hat{H}_B , will be, remembering that $\hat{X}'(0) = \hat{X}$,

$$\hat{X}' = e^{\hat{B}t} \hat{X} = e^{-i\frac{\hat{H}_B}{\hbar}t} \hat{X} e^{i\frac{\hat{H}_B}{\hbar}t}. \quad (32)$$

Equivalently, the action of $e^{\hat{S}t}$ on the density operator elements ρ_{ij} ($i, j = 1, 2$) will be determined by eq. (11), being the solution of the Lindblad superoperator with no environment. For $\hat{L}^{(S)} = \lambda \hat{\sigma}_z$, the solution will be given by [16]

$$\rho_{11}^{(z)}(t) = \rho_{11}^{(z)}(0), \quad (33)$$

$$\rho_{12}^{(z)}(t) = \rho_{12}^{(z)}(0) e^{-2\lambda^2 t} e^{-i2\omega_0 t}. \quad (34)$$

However, for $\hat{L}^{(S)} = \lambda \hat{\sigma}_x$, the solution is more complicated and will be given, in the $\hat{\sigma}_z$ eigenstates basis, by [26]

$$\left\{ \begin{aligned} \rho_{11}^{(z)}(t) &= \frac{1}{2} + \frac{2\rho_{11}^{(z)}(0) - 1}{2} e^{-2\lambda^2 t}, \\ \rho_{12}^{(z)}(t) &= e^{-\lambda^2 t} \left\{ \rho_{12}^{(z)}(0) \cosh \left(\sqrt{\lambda^4 - 4\omega_0^2} t \right) - \rho_{12}^{(z)}(0) \frac{i2\omega_0}{\sqrt{\lambda^4 - 4\omega_0^2}} \sinh \left(\sqrt{\lambda^4 - 4\omega_0^2} t \right) \right. \\ &\quad \left. + \frac{\lambda^2}{\sqrt{\lambda^4 - 4\omega_0^2}} \rho_{12}^{(z)*}(0) \sinh \left(\sqrt{\lambda^4 - 4\omega_0^2} t \right) \right\}. \end{aligned} \right. \quad (35)$$

Finally, it is necessary to change the basis to the eigenstates of the measurement apparatus, furnishing

$$\left\{ \begin{aligned} \rho_{11}^{(x)}(t) &= \frac{1}{2} + \text{Re} \left\{ \rho_{12}^{(z)}(t) \right\}, \\ \rho_{12}^{(x)}(t) &= -\frac{1}{2} + \rho_{11}^{(z)}(t) - i \text{Im} \left\{ \rho_{12}^{(z)}(t) \right\}. \end{aligned} \right. \quad (36)$$

In possession of these solutions, it is possible to solve the master equation under certain circumstances, which is done in the next two sections.

In our previous works [18,26,27], to obtain analytical solutions, we had considered only the system-environment interaction in the phase-damping format and, in the case when the Lindblad does not commute with that interaction, we had considered the particular situation when the frequency ω_0 and the environment temperature T are both zero. In the following sections, we will present numerical implementations without these restrictions and with the use of both kinds of interaction. For the environment, we adopt the initial thermal state:

$$\hat{\rho}_B = \frac{1}{Z_B} \prod_p e^{-\hbar\beta\omega_p \hat{b}_p^\dagger \hat{b}_p}, \quad Z_B = \prod_l \frac{1}{1 - e^{-\hbar\beta\omega_l}}, \quad (37)$$

with $\beta = \frac{1}{k_B T}$, where k_B is Boltzmann constant and T is the environmental temperature.

3 Phase-damping interaction

The case of phase-damping interaction was solved in two different manners: first, using the master equation given in the section above, valid for weak system-environment interaction. This is presented in the first subsection below. Afterward, we explain how the algorithm to numerically solve the Lindblad equation was written.

3.1 Solutions of the master equation

For the case of the phase-damping interaction,

$$\hat{H}_{SB} = \hbar\hat{\sigma}_z \sum_k \left(g_k \hat{b}_k^\dagger + g_k^* \hat{b}_k \right), \quad (38)$$

the treatment of the environment degrees of freedom was shown in [26], furnishing

$$\begin{aligned} \hat{P}\hat{G}(t)\hat{G}(t')\hat{P}\hat{\alpha}(t) &= \eta \int_0^\infty d\omega \omega e^{-\frac{\omega}{\omega_c}} \left\{ \coth\left(\frac{\hbar\beta\omega}{2}\right) \cos[\omega(t-t')] + i \sin[\omega(t-t')] \right\} \\ &\quad \times e^{-\hat{S}t} \left[\hat{\sigma}_z, \left\{ e^{\hat{S}(t-t')} \left[\left(e^{\hat{S}t'} \hat{R}(t) \right) \hat{\sigma}_z \right] \right\} \right] \otimes \hat{\rho}_B \\ &\quad + \eta \int_0^\infty d\omega \omega e^{-\frac{\omega}{\omega_c}} \left\{ \coth\left(\frac{\hbar\beta\omega}{2}\right) \cos[\omega(t-t')] - i \sin[\omega(t-t')] \right\} \\ &\quad \times e^{-\hat{S}t} \left[\left\{ e^{\hat{S}(t-t')} \left[\hat{\sigma}_z \left(e^{\hat{S}t'} \hat{R}(t) \right) \right] \right\}, \hat{\sigma}_z \right] \otimes \hat{\rho}_B, \end{aligned} \quad (39)$$

where we took the limit to the continuum by defining the spectral density function

$$J(\omega) = \sum_l |g_l|^2 \delta(\omega - \omega_l), \quad (40)$$

and employed an Ohmic spectral density (21).

3.1.1 The z -component measurement

The measurement of the z component, *i.e.*, $\hat{L}^{(S)} = \lambda\hat{\sigma}_z$ will furnish the (relatively) simple solutions [26]:

$$\begin{cases} \rho_{11}(t) = \rho_{11}(0), \\ \rho_{12}(t) = \rho_{12}(0) \left[\frac{\Gamma\left(\frac{1}{\omega_c\beta\hbar} + i\frac{t}{\beta\hbar}\right) \Gamma\left(\frac{1}{\omega_c\beta\hbar} - i\frac{t}{\beta\hbar}\right) \Gamma\left(\frac{1}{\omega_c\beta\hbar} + 1 + i\frac{t}{\beta\hbar}\right) \Gamma\left(\frac{1}{\omega_c\beta\hbar} + 1 - i\frac{t}{\beta\hbar}\right)}{\Gamma^2\left(\frac{1}{\omega_c\beta\hbar}\right) \Gamma^2\left(\frac{1}{\omega_c\beta\hbar} + 1\right)} \right]^{2\eta} e^{-2\lambda^2 t} e^{i2\omega_0 t}, \end{cases} \quad (41)$$

3.1.2 The x -component measurement

In the $\hat{\sigma}_z$ eigenbasis, as obtained in [26], the populations for $\hat{L}^{(S)} = \lambda\hat{\sigma}_x$ will be

$$\begin{cases} \rho_{11}^{(z)}(t) = \frac{2\rho_{11}^{(z)}(0) - 1}{2} e^{-2\lambda^2 t} + \frac{1}{2} \\ \rho_{12}^{(z)}(t) = \frac{e^{-\lambda^2 t}}{\Omega} \{ [\Omega \cosh(\Omega t) - i2\omega_0 \sinh(\Omega t)] r_{12}(t) + \lambda^2 \sinh(\Omega t) r_{21}(t) \} \end{cases}, \quad (42)$$

$$\Omega = \sqrt{\lambda^4 - 4\omega_0^2}, \quad (43)$$

where $r_{12}(t)$ and $r_{21}(t)$ are both solutions of the system

$$\begin{cases} \frac{d}{dt} r_{12}(t) = -4 \frac{\eta}{\Omega^3} \int_0^t dt' \int_0^\infty d\omega \omega e^{-\frac{\omega}{\omega_c}} \cos[\omega(t-t')] \coth\left(\frac{\beta\hbar\omega}{2}\right) [Q_1(t,t') r_{12}(t) + Q_2(t,t') r_{21}(t)] \\ \frac{d}{dt} r_{21}(t) = -4 \frac{\eta}{\Omega^3} \int_0^t dt' \int_0^\infty d\omega \omega e^{-\frac{\omega}{\omega_c}} \cos[\omega(t-t')] \coth\left(\frac{\beta\hbar\omega}{2}\right) [Q_2^*(t,t') r_{12}(t) + Q_1^*(t,t') r_{21}(t)] \end{cases}, \quad (44)$$

with

$$\begin{cases} Q_1(t,t') \equiv K_1(t) [K_1^*(t-t') K_1^*(t') - K_2(t-t') K_2(t')] + K_2(t) [K_2(t-t') K_1^*(t') - K_1(t-t') K_2(t')] \\ Q_2(t,t') \equiv K_1(t) [K_1^*(t-t') K_2(t') - K_2(t-t') K_1(t')] + K_2(t) [K_2(t-t') K_2(t') - K_1(t-t') K_1(t')] \end{cases}, \quad (45)$$

$$\begin{cases} K_1(t) \equiv \Omega \cosh(\Omega t) + i2\omega_0 \sinh(\Omega t) \\ K_2(t) \equiv \lambda^2 \sinh(\Omega t) \end{cases}. \quad (46)$$

3.2 Numerical solution of the Lindblad equation

To compare the semi-analytical results of the hybrid master equation with the numerical simulations of the Lindblad equation, we employed the same superoperator-splitting method described in a previous article [26]. A few adaptations were necessary for the inclusion of non-vanishing ω_0 and temperature T . We shall approach the introduction of these two parameters separately in the subsections that follow.

3.2.1 Introduction of ω_0

As stated in eq. (41) of [26], the final state of the system subject to phase noise and a perpendicular measurement can be calculated using the superoperator-splitting method through the algorithm:

$$\begin{pmatrix} \rho_{12}^{(z)}(t) \\ \rho_{21}^{(z)}(t) \end{pmatrix} = e^{-\lambda^2 t} \sum_{q_1 \in \{-1,1\}} \dots \sum_{q_N \in \{-1,1\}} \prod_{n=1}^N [A_{q_n}(\Delta t)] \text{Tr}_B \left\{ \prod_{n=1}^N [\hat{K}_{q_n}(\Delta t)] \hat{\rho}_B \right\} \begin{pmatrix} \rho_{12}^{(z)}(0) \\ \rho_{21}^{(z)}(0) \end{pmatrix}, \quad (47)$$

where $t = N\Delta t$ and the superoperators $\hat{K}_q(\Delta t)$ satisfy, when the noise is along the \hat{z} direction,

$$\hat{K}_q(\Delta t) \hat{X} \equiv e^{-i \sum_k \omega_k (\hat{b}_k + qg_k/\omega_k)^\dagger (\hat{b}_k + qg_k/\omega_k) \Delta t} \hat{X} e^{i \sum_k \omega_k (\hat{b}_k - qg_k/\omega_k)^\dagger (\hat{b}_k - qg_k/\omega_k) \Delta t},$$

and the $A_{q_n}(\Delta t)$ are 2×2 matrices that depend on the solution of the noiseless Lindblad equation, *i.e.*

$$\frac{d}{dt} \rho(t) = -i\omega_0 [\sigma_z, \rho(t)] + \lambda^2 [\sigma_x \rho(t) \sigma_x - \rho(t)].$$

In our previous article we chose $\omega_0 = 0$, thus rendering the solution of the equation in the eigenbasis of σ_z simply

$$\begin{pmatrix} \rho_{12}^{(z)}(\Delta t) \\ \rho_{21}^{(z)}(\Delta t) \end{pmatrix} = e^{-\lambda^2 \Delta t} A_+^{(0)}(\Delta t) \begin{pmatrix} \rho_{12}^{(z)}(0) \\ \rho_{21}^{(z)}(0) \end{pmatrix} + e^{-\lambda^2 \Delta t} A_-^{(0)}(\Delta t) \begin{pmatrix} \rho_{12}^{(z)}(0) \\ \rho_{21}^{(z)}(0) \end{pmatrix},$$

where the matrices $A_{\pm}^{(0)}(\Delta t)$ are

$$A_{+}^{(0)}(\Delta t) = \begin{pmatrix} \cosh(\lambda^2 \Delta t) & \sinh(\lambda^2 \Delta t) \\ 0 & 0 \end{pmatrix}, \quad A_{-}^{(0)}(\Delta t) = \begin{pmatrix} 0 & 0 \\ \sinh(\lambda^2 \Delta t) & \cosh(\lambda^2 \Delta t) \end{pmatrix}.$$

In this new situation where $\omega_0 \neq 0$, the solution for the coherences will require these matrices instead:

$$A_{+}(\Delta t) = \frac{1}{\Omega} \begin{pmatrix} \Omega \cosh(\Omega \Delta t) - 2i\omega_0 \sinh(\Omega \Delta t) & \lambda^2 \sinh(\Omega \Delta t) \\ 0 & 0 \end{pmatrix},$$

$$A_{-}(\Delta t) = \frac{1}{\Omega} \begin{pmatrix} 0 & 0 \\ \lambda^2 \sinh(\Omega \Delta t) & \Omega \cosh(\Omega \Delta t) + 2i\omega_0 \sinh(\Omega \Delta t) \end{pmatrix},$$

where $\Omega \equiv \sqrt{\lambda^4 - 4\omega_0^2}$. It is easy to verify that, when $\omega_0 = 0$, $\Omega = \lambda^2$, the original matrices $A_{\pm}^{(0)}(\Delta t)$ are recovered.

The full expression of the algorithm in eq. (47) requires a product of N such matrices for each term of the N summations. We can reduce the computational overhead by simplifying analytically the results before writing the program. Following the method employed in the previous article, we first define the functions

$$c_{+}(\Delta t) \equiv \cosh(\Omega \Delta t) - 2i\omega_0 \frac{1}{\Omega} \sinh(\Omega \Delta t),$$

$$c_{-}(\Delta t) \equiv \lambda^2 \frac{1}{\Omega} \sinh(\Omega \Delta t),$$

so that the products of these matrices can be written as

$$A_{q_n}(\Delta t)A_{q_{n+1}}(\Delta t) = c_{q_n q_{n+1}}^{q_n}(\Delta t)(\sigma_x)^{(1-q_n q_{n+1})/2}A_{q_{n+1}}(\Delta t),$$

where a minus sign as a superscript in the $c(\Delta t)$ represents taking its complex conjugate ($c^{+} = c$, $c^{-} = c^*$).

Proceeding iteratively with all the N products, we find

$$\prod_{n=1}^N [A_{q_n}(\Delta t)] = \prod_{n=1}^{N-1} c_{q_n q_{n+1}}^{q_n}(\Delta t)(\sigma_x)^{\sum_{n=1}^{N-1} (1-q_n q_{n+1})/2}A_{q_N}(\Delta t).$$

Noting additionally that $(\sigma_x)^{(1-q_1 q_2)/2}(\sigma_x)^{(1-q_2 q_3)/2} = (\sigma_x)^{1-q_2(q_1+q_3)/2} = (\sigma_x)^{(1-q_1 q_3)/2}$, the product simplifies even further. Back to eq. (47),

$$\begin{pmatrix} \rho_{12}(N\Delta t) \\ \rho_{21}(N\Delta t) \end{pmatrix} = e^{-\lambda^2(N\Delta t)} \sum_{q_1 \in \{-1,1\}} \dots \sum_{q_N \in \{-1,1\}} \left[\prod_{n=1}^{N-1} c_{q_n q_{n+1}}^{q_n}(\Delta t) \right] (\sigma_x)^{(1-q_1 q_N)/2}$$

$$\times A_{q_N}(\Delta t) \prod_{m,n=1}^N \left\{ 1 + \frac{2(\omega_c \Delta t)^{-2} + (1 - 2|m - n|^2)}{[(\omega_c \Delta t)^{-2} + |m - n|^2]^2} \right\}^{-\eta q_m q_n} \begin{pmatrix} \rho_{12}(0) \\ \rho_{21}(0) \end{pmatrix},$$

where we have already replaced the trace for its result at zero temperature, given in appendix G of [26]. In the next section, we will see how this trace is modified for the case when $T > 0$.

3.2.2 Introduction of T

In the case when the system has some temperature $T > 0$, the trace we have to take is

$$\text{Tr}_B \left\{ \prod_{n=1}^N [\hat{K}_{q_n}(\Delta t)] \frac{e^{-\beta \hbar \sum_k \omega_k \hat{b}_k^\dagger \hat{b}_k}}{Z} \right\}.$$

We will employ once again the basis of coherent states to take the trace. When acting upon the superoperator $\hat{K}_{q_n}(\Delta t)$, coherent-state bras and kets result in:

$$\bigotimes_k \langle \alpha'_k | \hat{K}_{q_n}(\Delta t) \hat{X} \bigotimes_k | \alpha_k \rangle = \bigotimes_k \langle e^{i\omega_k \Delta t} \alpha'_k + (e^{i\omega_k \Delta t} - 1)G_k | \hat{X} \bigotimes_k | e^{i\omega_k \Delta t} \alpha_k - (e^{i\omega_k \Delta t} - 1)G_k \rangle$$

$$\times e^{\sum_k (G_k^* (1 - e^{i\omega_k \Delta t})(\alpha_k + \alpha'_k) - G_k (1 - e^{-i\omega_k \Delta t})(\alpha_k + \alpha'_k)^*)/2},$$

where we have defined

$$G_k \equiv q \frac{g_k}{\omega_k}.$$

Repeating the procedure N times, we find:

$$\begin{aligned} \bigotimes_k \langle \alpha_k | \prod_{n=1}^N [\hat{K}_{q_n}(\Delta t)] \rho_B(0) \bigotimes_k | \alpha_k \rangle &= \bigotimes_k \left\langle e^{iN\omega_k \Delta t} \left[\alpha_k + \sum_{n=1}^N (e^{i\omega_k \Delta t} - 1) G_{n,k} \right] \right| \\ &\times \frac{e^{-\beta \hbar \sum_k \omega_k \hat{b}_k^\dagger \hat{b}_k}}{Z} \bigotimes_k \left| e^{iN\omega_k \Delta t} \left[\alpha_k - \sum_{n=1}^N (e^{i\omega_k \Delta t} - 1) G_{n,k} \right] \right\rangle \\ &\times e^{\sum_{n,k} (G_{n,k}^* e^{-i\omega_k \Delta t} (1 - e^{i\omega_k \Delta t}) \alpha_k - G_{n,k} e^{i\omega_k \Delta t} (1 - e^{-i\omega_k \Delta t}) \alpha_k^*)}, \end{aligned}$$

where

$$G_{n,k} \equiv e^{-in\omega_k \Delta t} q_n \frac{g_k}{\omega_k}$$

and the \hat{X} operator has been replaced by the initial density matrix of the environment. Its action on the coherent state yields

$$\begin{aligned} e^{-\beta \hbar \omega_k \hat{b}_k^\dagger \hat{b}_k} \left| e^{iN\omega_k \Delta t} \left[\alpha_k - \sum_{n=1}^N (e^{i\omega_k \Delta t} - 1) G_{n,k} \right] \right\rangle &= \left| e^{-\beta \hbar \omega_k} e^{iN\omega_k \Delta t} \left[\alpha_k - \sum_{n=1}^N (e^{i\omega_k \Delta t} - 1) G_{n,k} \right] \right\rangle \\ &\times e^{-\frac{1}{2}(1 - e^{-2\beta \hbar \omega_k}) \left| \alpha_k - \sum_{n=1}^N (e^{i\omega_k \Delta t} - 1) G_{n,k} \right|^2}. \end{aligned}$$

Therefore,

$$\begin{aligned} \bigotimes_k \langle \alpha_k | \prod_{n=1}^N [\hat{K}_{q_n}(\Delta t)] \rho_B(0) \bigotimes_k | \alpha_k \rangle &= \prod_k \left(\frac{1}{1 - e^{-\beta \hbar \omega_k}} \right)^{-1} \exp \left\{ -(1 - e^{-\beta \hbar \omega_k}) |\alpha_k|^2 \right\} \\ &\times \exp \left\{ -(1 + e^{-\beta \hbar \omega_k}) \sum_{n=1}^N 2i \operatorname{Im} \left[G_{n,k}^* (1 - e^{-i\omega_k \Delta t}) \alpha_k \right] \right\} \\ &\times \exp \left\{ -(1 + e^{-\beta \hbar \omega_k}) \left| \sum_{n=1}^N (e^{i\omega_k \Delta t} - 1) G_{n,k} \right|^2 \right\}. \end{aligned}$$

Taking the trace, we find ourselves integrating over the complex plane:

$$\begin{aligned} \operatorname{Tr} \dots &= \prod_k \left(\frac{1}{1 - e^{-\beta \hbar \omega_k}} \right)^{-1} \frac{1}{\pi} \\ &\times \int_{-\infty}^{\infty} dx \exp \left\{ -(1 - e^{-\beta \hbar \omega_k}) x^2 \right\} \exp \left\{ -(1 + e^{-\beta \hbar \omega_k}) 2i \operatorname{Im} \left[\sum_{n=1}^N G_{n,k}^* (1 - e^{-i\omega_k \Delta t}) \right] x \right\} \\ &\times \int_{-\infty}^{\infty} dy \exp \left\{ -(1 - e^{-\beta \hbar \omega_k}) y^2 \right\} \exp \left\{ -(1 + e^{-\beta \hbar \omega_k}) 2i \operatorname{Re} \left[\sum_{n=1}^N G_{n,k}^* (1 - e^{-i\omega_k \Delta t}) \right] y \right\} \\ &\times \exp \left\{ -(1 + e^{-\beta \hbar \omega_k}) \left| \sum_{n=1}^N (e^{i\omega_k \Delta t} - 1) G_{n,k} \right|^2 \right\}. \end{aligned}$$

These are integrals of Gaussians, which can be solved by

$$\int_{-\infty}^{\infty} dx e^{-ax^2} e^{-2i \operatorname{Im}(b)x} \int_{-\infty}^{\infty} dy e^{-ay^2} e^{-2i \operatorname{Re}(b)y} = \frac{\pi}{a} e^{-|b|^2/a},$$

yielding the result of, after taking the continuous limit of frequencies, and Ohmic spectral density (21):

$$\operatorname{Tr} \dots = \exp \left\{ -8\eta \sum_{m,n=1}^N q_m q_n \int_0^{\infty} d\omega e^{-\omega/\omega_c} \frac{e^{-i(m-n)\omega \Delta t}}{\omega} \coth \left(\frac{\hbar \beta \omega}{2} \right) \sin^2 \left(\frac{\omega t}{2} \right) \right\}.$$

This final expression clearly recovers the integral given in appendix G of our previous article [26] in the limit when $T \rightarrow 0$, because

$$\lim_{\beta \rightarrow \infty} \coth \left(\frac{\hbar\beta\omega}{2} \right) = 1.$$

Moreover, it reduces to the expression of decoherence in a finite-temperature (eq. (18) of ref. [31]) environment when we take just one step ($N = 1$):

$$\exp \left\{ -8\eta \int_0^\infty d\omega \frac{e^{-\omega/\omega_c}}{\omega} \coth \left(\frac{\hbar\beta\omega}{2} \right) \sin^2 \left(\frac{\omega t}{2} \right) \right\}.$$

4 Amplitude-damping interaction

The amplitude-damping interaction —which, here, is only solved using the master equation— is described by the Jaynes-Cummings interaction Hamiltonian:

$$\hat{H}_{SB} = \hbar \sum_k \left(g_k \hat{b}_k \hat{\sigma}_+ + g_k^* \hat{b}_k^\dagger \hat{\sigma}_- \right), \tag{48}$$

where

$$\begin{aligned} \hat{\sigma}_+ &= \begin{pmatrix} 0 & 1 \\ 0 & 0 \end{pmatrix}, \\ \hat{\sigma}_- &= \begin{pmatrix} 0 & 0 \\ 1 & 0 \end{pmatrix}. \end{aligned} \tag{49}$$

The partial trace for the environmental degrees of freedom, following the procedures already shown in [18,26], furnish:

$$\begin{aligned} \hat{P}\hat{G}(t)\hat{G}(t')\hat{P}\hat{\alpha}(t) &= \eta \int_0^\infty d\omega \omega e^{-\frac{\omega}{\omega_c}} \frac{e^{-i\omega(t-t')}}{e^{\hbar\beta\omega} - 1} e^{-\hat{S}t} \left[\hat{\sigma}_+, \left\{ e^{\hat{S}(t-t')} \left[(e^{\hat{S}t'} \hat{R}(t)) \hat{\sigma}_- \right] \right\} \right] \hat{\rho}_B \\ &+ \eta \int_0^\infty d\omega \omega e^{-\frac{\omega}{\omega_c}} \frac{e^{i\omega(t-t')}}{1 - e^{-\hbar\beta\omega}} e^{-\hat{S}t} \left[\hat{\sigma}_-, \left\{ e^{\hat{S}(t-t')} \left[(e^{\hat{S}t'} \hat{R}(t)) \hat{\sigma}_+ \right] \right\} \right] \hat{\rho}_B \\ &+ \eta \int_0^\infty d\omega \omega e^{-\frac{\omega}{\omega_c}} \frac{e^{i\omega(t-t')}}{e^{\hbar\beta\omega} - 1} e^{-\hat{S}t} \left[\left\{ e^{\hat{S}(t-t')} \left[\hat{\sigma}_+ (e^{\hat{S}t'} \hat{R}(t)) \right] \right\}, \hat{\sigma}_- \right] \hat{\rho}_B \\ &+ \eta \int_0^\infty d\omega \omega e^{-\frac{\omega}{\omega_c}} \frac{e^{-i\omega(t-t')}}{1 - e^{-\hbar\beta\omega}} e^{-\hat{S}t} \left[\left\{ e^{\hat{S}(t-t')} \left[\hat{\sigma}_- (e^{\hat{S}t'} \hat{R}(t)) \right] \right\}, \hat{\sigma}_+ \right] \hat{\rho}_B. \end{aligned} \tag{50}$$

where we are employing the Ohmic spectral density (21).

4.1 The z-component measurement

For $\hat{L}^{(S)} = \lambda \hat{\sigma}_z$, the treatment of (50) and its substitution in (14) will furnish, for $\hat{R}(t)$,

$$\left\{ \begin{aligned} \frac{d}{dt} R_{11} &= 2R_{22}(t)\eta \int_0^t d\tau \int_0^\infty d\omega \frac{\omega e^{-\frac{\omega}{\omega_c}}}{e^{\hbar\beta\omega} - 1} e^{-2\lambda^2\tau} \cos [(2\omega_0 - \omega)\tau] \\ &- 2R_{11}(t)\eta \int_0^t d\tau \int_0^\infty d\omega \frac{\omega e^{-\frac{\omega}{\omega_c}}}{1 - e^{-\hbar\beta\omega}} e^{-2\lambda^2\tau} \cos [(2\omega_0 - \omega)\tau] \\ R_{12}(t) &= R_{12}(0) \exp \left\{ -\eta \int_0^t dt' \int_0^\infty d\omega \omega e^{-\frac{\omega}{\omega_c}} \frac{e^{2\lambda^2 t'} e^{i(2\omega_0 - \omega)t'} - 1}{2\lambda^2 + i(2\omega_0 - \omega)} \coth \left(\frac{\hbar\beta\omega}{2} \right) \right\} \end{aligned} \right. , \tag{51}$$

remembering that $R_{11}(t) + R_{22}(t) = 1$ and $R_{12}(t) = R_{21}^*(t)$.

4.2 The x-component measurement

For $\hat{L}^{(S)} = \lambda \hat{\sigma}_x$, as expected, the expressions will be more complex, furnishing,

$$\left\{ \begin{array}{l} \frac{d}{dt} R_{11} = 2R_{11}(t)e^{2\lambda^2 t} \int_0^t dt' \int_0^\infty d\omega J(\omega) \operatorname{Re} \left\{ a_2(t')b_1^*(t-t') \frac{e^{-i\omega(t-t')}}{e^{\hbar\beta\omega} - 1} - a_1(t')b_1(t-t') \frac{e^{i\omega(t-t')}}{1 - e^{-\hbar\beta\omega}} \right\} \\ \quad + 2R_{22}(t)e^{2\lambda^2 t} \int_0^t dt' \int_0^\infty d\omega J(\omega) \operatorname{Re} \left\{ a_1(t')b_1^*(t-t') \frac{e^{-i\omega(t-t')}}{e^{\hbar\beta\omega} - 1} - a_2(t')b_1(t-t') \frac{e^{i\omega(t-t')}}{1 - e^{-\hbar\beta\omega}} \right\} \\ \frac{d}{dt} R_{12} = -R_{12}(t) \int_0^t dt' \int_0^\infty d\omega J(\omega) e^{-2\lambda^2(t-t')} \coth\left(\frac{\hbar\beta\omega}{2}\right) [b_1(-t)b_1(t')e^{-i\omega(t-t')} + b_2(-t)b_2(t')e^{i\omega(t-t')}] \\ \quad - R_{21}(t) \int_0^t dt' \int_0^\infty d\omega J(\omega) e^{-2\lambda^2(t-t')} \coth\left(\frac{\hbar\beta\omega}{2}\right) [b_1(-t)b_2(t')e^{-i\omega(t-t')} + b_1^*(t')b_2(-t)e^{i\omega(t-t')}] \end{array} \right. , \quad (52)$$

where

$$\left\{ \begin{array}{l} a_1(t) = \frac{1 + e^{-2\lambda^2 t}}{2} \\ a_2(t) = \frac{1 - e^{-2\lambda^2 t}}{2} \\ b_1(t) = \frac{e^{-\lambda^2 t}}{\Omega} [\Omega \cosh(\Omega t) - i2\omega_0 \sinh(\Omega t)] \\ b_2(t) = \frac{\lambda^2}{\Omega} e^{-\lambda^2 t} \sinh(\Omega t) \end{array} \right. , \quad (53)$$

remembering that again $R_{11}(t) + R_{22}(t) = 1$ and $R_{12}(t) = R_{21}^*(t)$. After \hat{R} has been found, it is still necessary a change of basis to find the density operator in the eigenbasis of $\hat{\sigma}_x$, as in the discussion of eq. (44).

5 Results and analysis

After laying down the methods for obtaining the solutions, we now can observe what they look like in graphs. There are four parameters to be analysed:

- λ , the coupling strength between the system and the measuring apparatus;
- η , the coupling strength between the system and the environment;
- ω_0 , the splitting, in frequency units, between the two energy levels of the principal system, henceforth called the natural frequency of the system;
- T , the environment temperature, also expressed in terms of $\beta = 1/k_B T$, where k_B is the Boltzmann constant. Note that $T = 0$ corresponds to the limit in which $\beta \rightarrow \infty$.

In this section, we observe how the measurement, represented by λ , affects the evolution of the system for different values of the other three parameters η , ω_0 , and β .

It may be noted that in some cases the natural frequency of the system is taken as zero ($\omega_0 = 0$). This is not simply a manner of simplifying the calculations, despite certainly having this advantage. This is equivalent to turning off the natural evolution of the two-level system, as in the case of a memory qubit. It is, therefore, a situation of relevance in the context of quantum computation, because quantum memories are necessary to the proper synchronization of the internal processes of a quantum computer [32].

5.1 Phase damping

The phase damping channel merely causes the loss of coherence in the basis of $\hat{\sigma}_z$, thus having an effect similar to a measurement of this observable. It does not affect the populations in this basis and, therefore, the outcome of the $\hat{\sigma}_z$ measurement remains unchanged. However, as it makes the coherences disappear, it does affect the outcomes of the measurement of $\hat{\sigma}_x$, for example. In this case, as the coherences in the original basis vanish, the populations in the basis of $\hat{\sigma}_x$ approach $1/2$, thus destroying any information that we initially could obtain from a measurement of that observable.

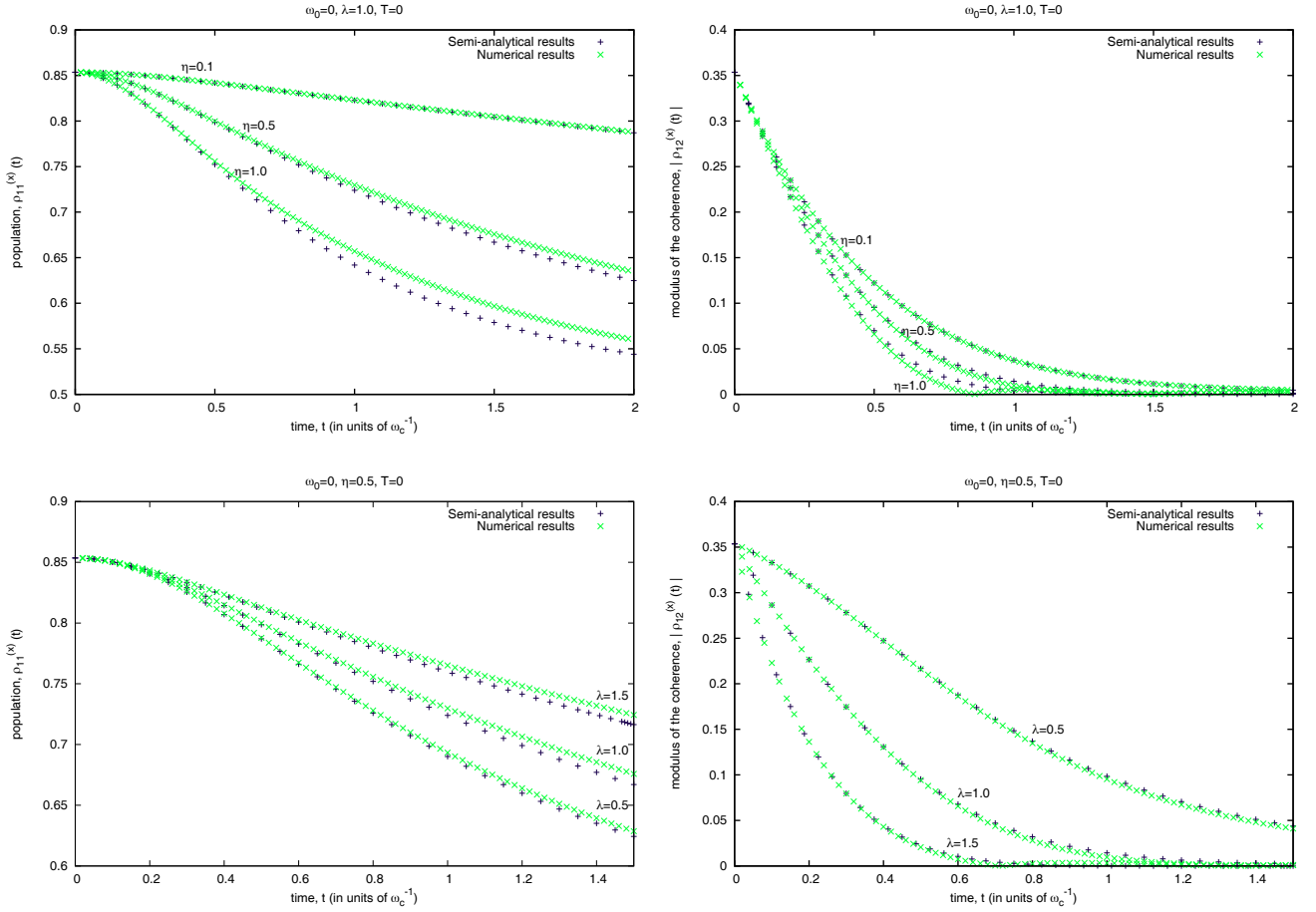


Fig. 1. Populations and coherences in the eigenbasis of the measured observable for $\omega_0 = 0$ and $T = 0$. In this case the conclusions are the same as those presented in ref. [26].

5.1.1 The z -component measurement

Equation (41) is the complete analytical solution for this case, and it includes all the parameters of our problem. For this case, we can see [26] that:

- the populations are constant in time, for any value of the parameters ω_0 , λ , η , and T ;
- the moduli of the coherences are independent of ω_0 and an increase in the other parameters just makes the decay more intense.

These results are expected, because the frequency ω_0 only affects the phases of the coherences, and both the measuring apparatus and the environment are responsible for measuring the system in the eigenbasis of $\hat{\sigma}_z$, thus causing decoherence. The only new result is that the environmental temperature also helps to increase the decoherence, an effect not unlike those found in other works that did not involve the measuring apparatus [31].

5.1.2 The x -component measurement

While in [26] we had to make the restrictions $\omega_0 = 0$ and $T = \frac{1}{k_B\beta} = 0$ in (42)–(46) to obtain analytical solutions, here the equation is solved numerically to analyse the influence of all parameters.

Figure 1 reproduces the analytical results of [26,27] for $\omega_0 = 0$ and $T = 0$, namely, that the change in value of the population, caused by the interaction with the environment and therefore increased with η , is attenuated by the system-apparatus coupling λ . Regarding the coherences, which tend to zero in absolute value, we are able to establish a time for the measurement process to reach completion. In [27] we have found, for this specific situation, an upper limit for the measurement duration:

$$t_M = -\frac{1}{2\lambda^2} \ln f, \tag{54}$$

where f is an arbitrary fraction of the initial value of the moduli of the coherences ($0 < f < 1$).

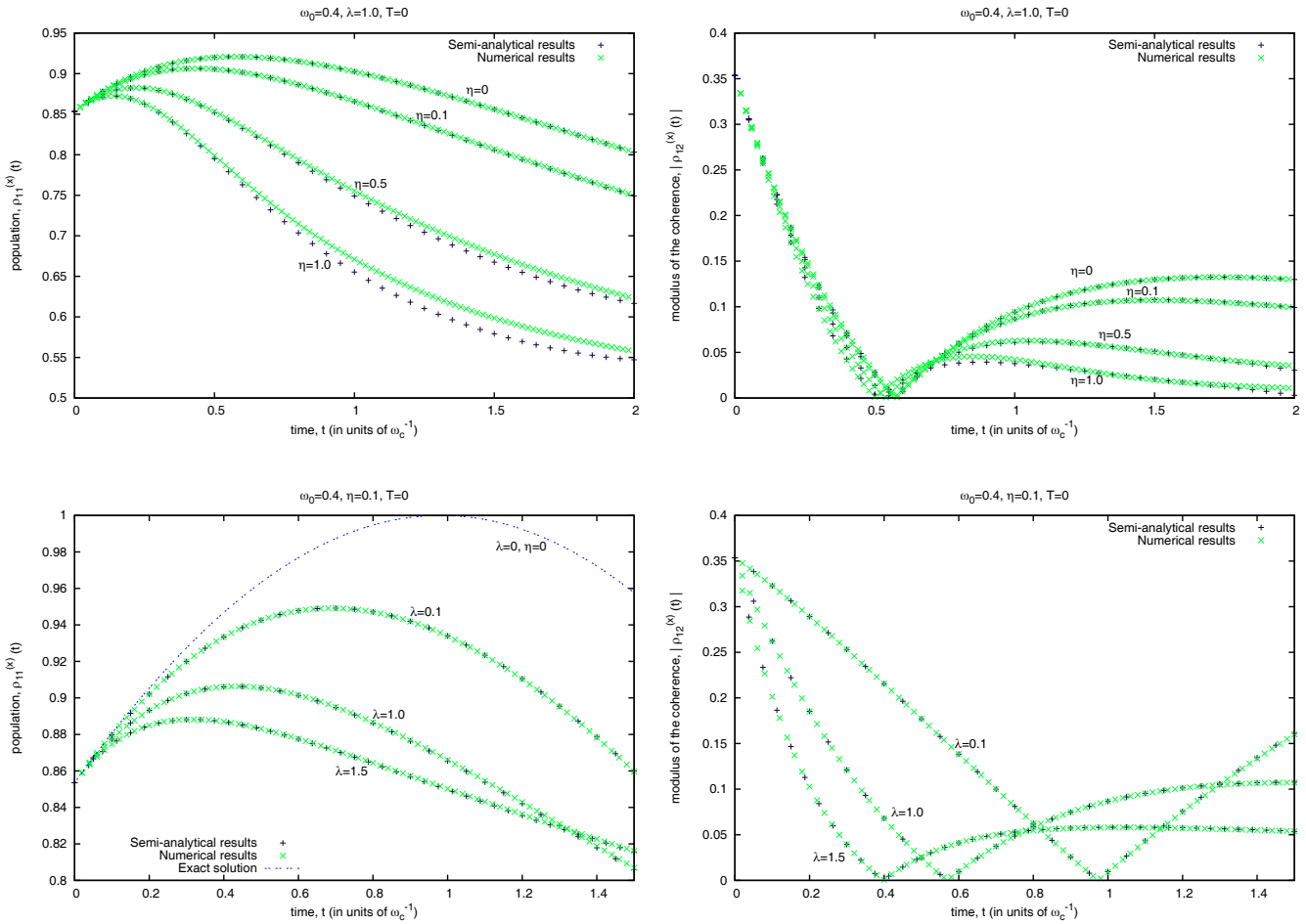


Fig. 2. Curves referring to the population in the eigenbasis of the measured observable, considering many values of λ and η , and a non-zero value of ω_0 , while keeping $T = 0$.

Moreover, the comparison between the solution of the master equation and the numerical results obtained from the superoperator-splitting procedure are in good agreement for low values of η , but the two curves depart more and more from each other as the strength of the coupling increases. This is due to the fact that the master equation is a lower-order approximation valid only in the limit of small η . For higher values of η , the approximation fails.

After reproducing the numerical results known to the analytical approach, we add a new parameter: the system frequency, ω_0 . Figure 2 is equivalent to fig. 1, now considering a non-zero value for ω_0 .

From fig. 2, we note that the increase of the system frequency changes the behavior of the populations, which is no longer monotonic. In the time interval considered here, we are able to observe that the populations oscillate. From fig. 2(c), we observe that, the lower the value of λ , the closer is the evolution of the populations to the unperturbed case (dashed lines). This might mislead us into thinking that the finite-time measurement is less efficient than the instantaneous in this case. This notion is false, however, because the state we want to measure is the one at the instant $t = 0$, when the measurement apparatus is turned on. In general, the curve with the highest λ is still the one that conserves the population closest to its initial value for most of the time, meaning that the measurement protects the system from the environment and prevents its inherent evolution, as in the Zeno effect [33].

For the moduli of the coherences, the monotonic behavior is likewise eliminated. However, while for the populations we found a point of maximum, here we find also a point of minimum at zero, where the coherences change sign and their moduli bounce upwards. As the system-environment coupling strength η becomes more intense, the time when the magnitude of the coherences is zero becomes smaller, while keeping the moduli in general closer to zero even after the point of minimum. A similar effect is observed for λ , which is expected from the fact that both the apparatus and the environment interactions are contributing to the decoherence.

Now, we will consider the effects of another parameter neglected in our previous works [26,27]: the temperature of the environment. Figure 3 shows the behavior of populations and coherences for a fixed value of the strength of the coupling between the system and the environment when the system has zero frequency ω_0 , in the case in which

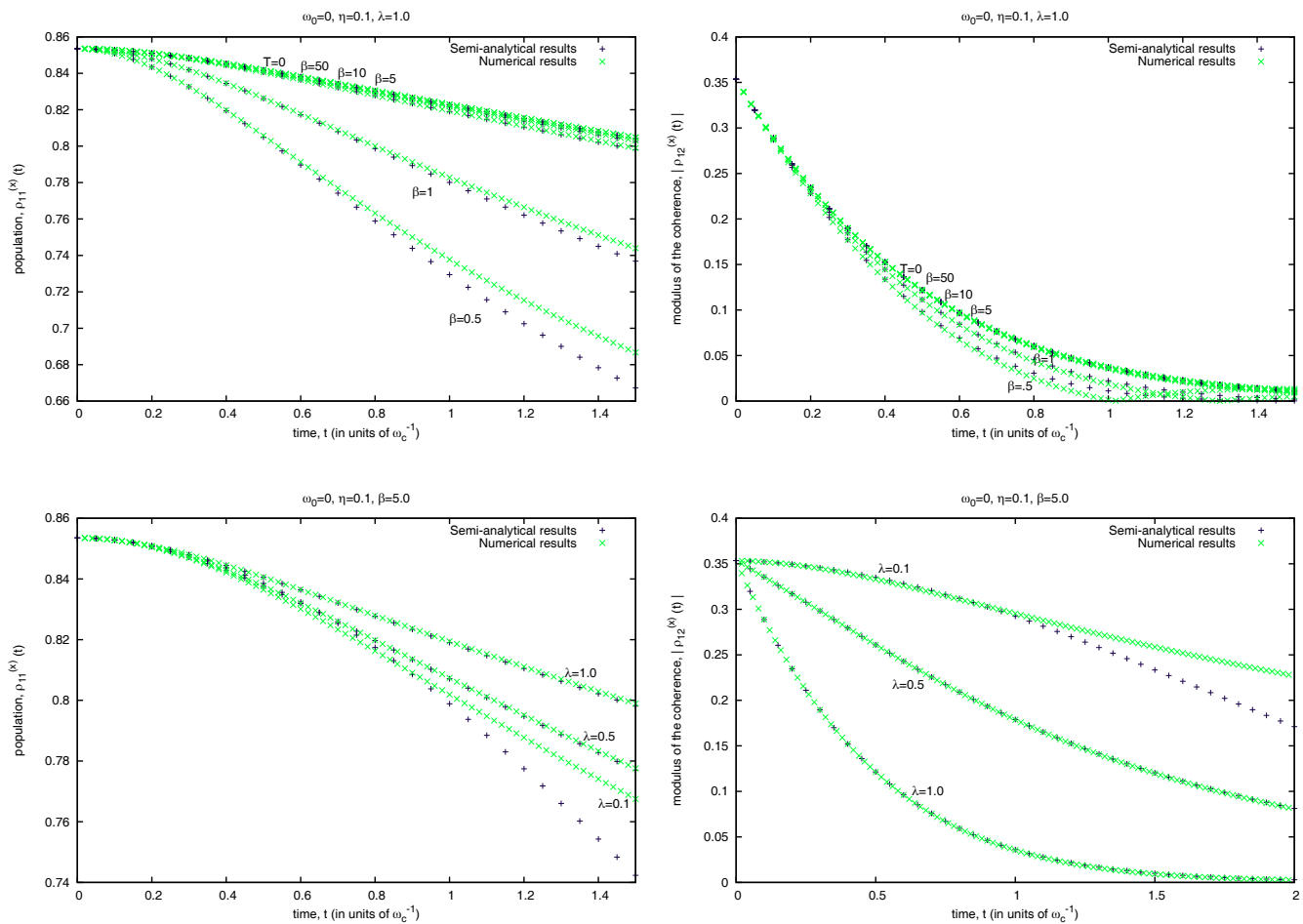


Fig. 3. Curves for the analysis of the effects of the environmental temperature for $\omega_0 = 0$.

we vary λ and T . It is possible to observe, for populations, that, while an increase of the temperature makes the deleterious effects of the environment more pronounced, a similar increase in λ is capable of compensating for these effects, thus attenuating the rate of population change. Therefore, we can conclude that the simple addition of the environment temperature to the model does not change our previously published conclusions about state protection and measurement error [26,27].

For the moduli of the coherences, we still have the same effects of faster decrease for higher λ , as seen in fig. 3(d). The only new fact is that the environmental finite temperature has a similar effect to η in making the coherences approach zero.

Ending the analysis of phase-damping interaction, fig. 4 shows several curves with fixed and non-zero environment parameters η and T , varying λ . As in the previous cases, here we once again verify that the measurement has a twofold effect on the system: it attenuates the changes in the populations and increases the rate at which the coherences vanish, confirming, so far, the conclusions of our previous works [26,27].

5.2 Amplitude damping

The amplitude-damping system-environment interaction differs from phase-damping by not simply being an agent of decoherence. This kind of interaction causes the decay of the excited state $|1\rangle$ to the ground state $|2\rangle$, thus resulting in the gradual decrease of the population $\rho_{11}(t)$ until its complete disappearance.

However, if the temperature is not zero, as in many cases we are treating here, the repopulation of the excited state by the environment will result in a final equilibrium population that lies above zero. This value, proportional to the Boltzmann weight $e^{-\hbar\beta\omega_0}$, increases with temperature (with more energy available, the environment will more easily repopulate the excited state) but decreases with ω_0 (the higher the energy difference, the more difficult it is to repopulate). For $T > 0$ and $\omega_0 = 0$, both populations assume a final value of 0.5, as will be seen below.

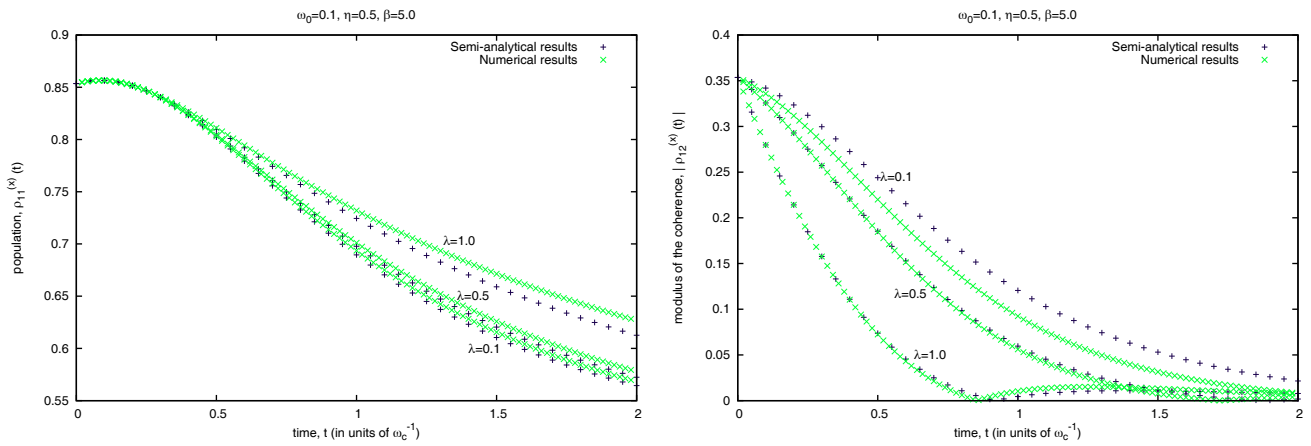


Fig. 4. Simultaneous influence of the frequency of the system and the environmental temperature.

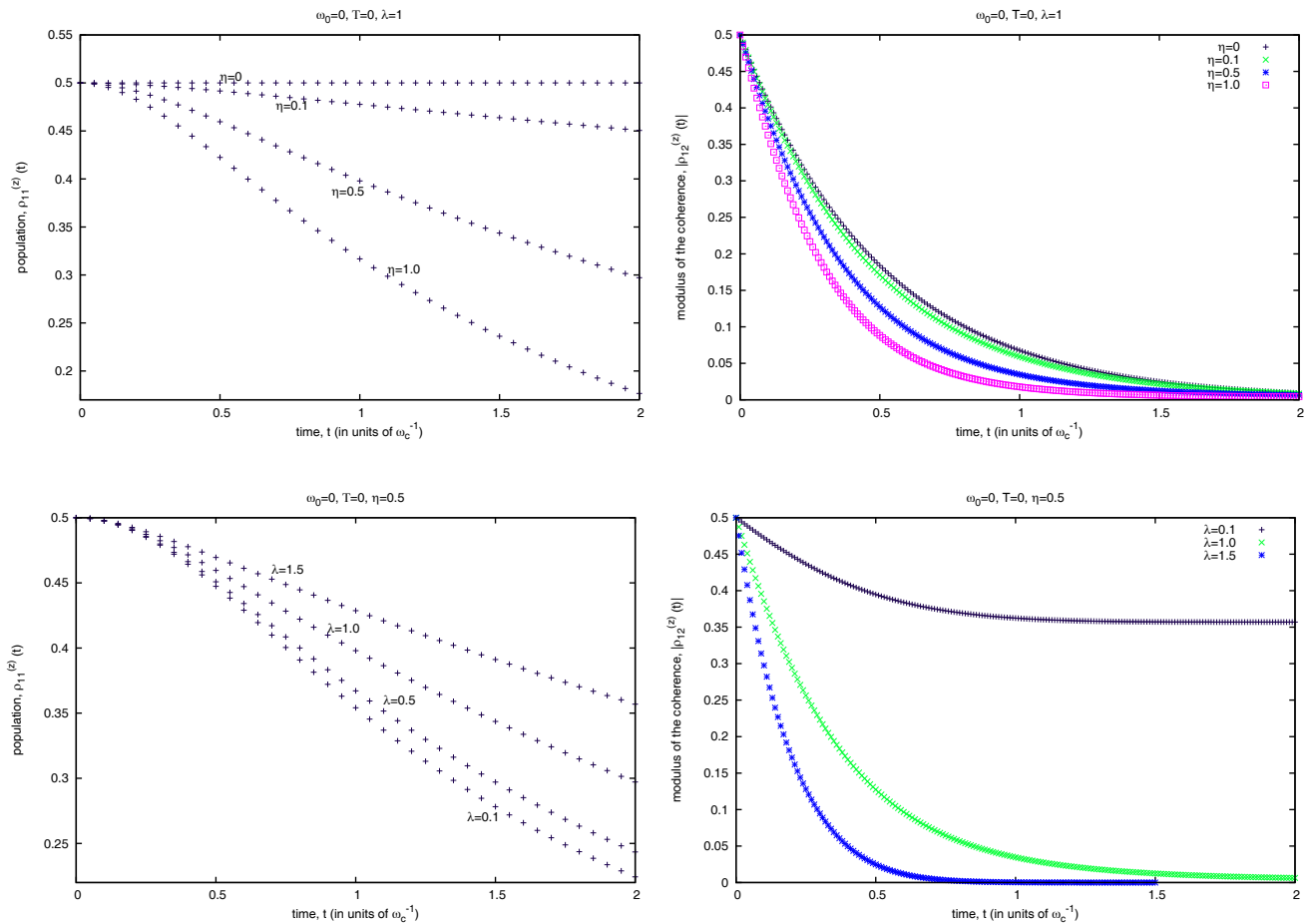


Fig. 5. Curves for the amplitude-damping interaction, during a measurement of the z -component, considering different values of λ and η , but with $T = \omega_0 = 0$.

5.2.1 The z -component measurement

Contrary to the phase-damping case, amplitude-damping changes the value of the populations in the eigenbasis of $\hat{\sigma}_z$, allowing us to observe interesting effects even in this case. Figure 5 shows curves for the population and modulus of the coherence considering several values of η and λ , but still with temperature T and frequency ω_0 turned off.

The strengthening of the system-environment coupling η causes a more intense decrease of the population that can be compensated by an increase in the system-measurement apparatus coupling λ . This causes a reduction of the rate of decay analogous to the phase-damping interaction with an x -component measurement. For the coherence, the increase

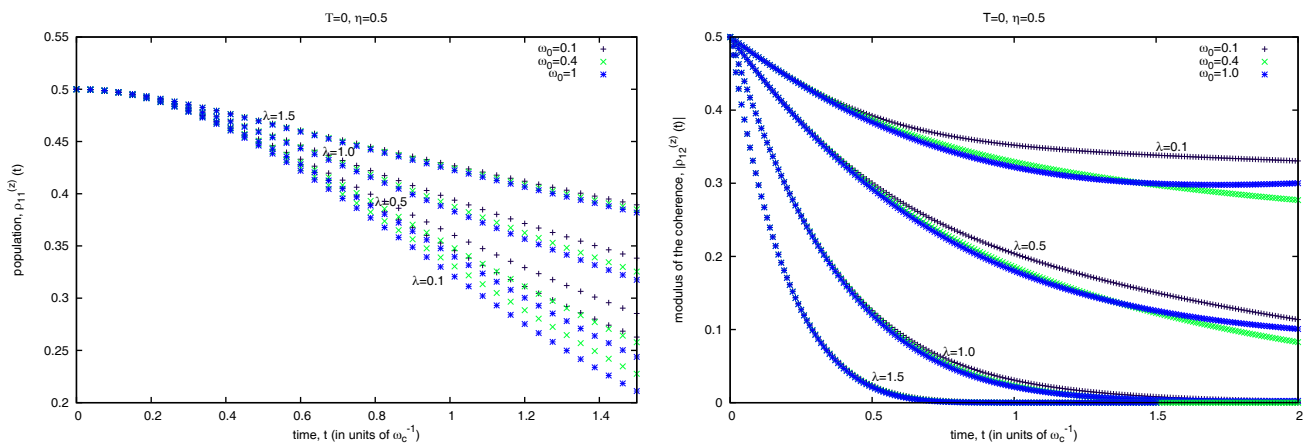


Fig. 6. Curves for the population and modulus of the coherence considering different values of λ , with non-zero ω_0 .

of η or λ causes a more intense decrease of the modulus. Therefore, the conclusions from [26,27] and the previous section of this article remain valid here, despite our having changed not simply the system-environment interaction but the measured component too.

Let us introduce the system frequency, ω_0 . From fig. 6, we note this parameter does not change significantly the population and coherence behavior and, then, we have the same conclusions about the effects of λ and η .

The coherences have their behavior governed mainly by λ , which, as always, makes the moduli go faster to zero while keeping the population closer to its original value. For both variables, a larger system frequency ω_0 results in a more intense decrease. For the populations, this fact can be easily explained because an increase in the difference between the energy levels makes repopulation more difficult. Then, ω_0 and λ have compensating effects.

With the introduction of the environmental temperature T (fig. 7), we note that, as expected, if we keep T constant, we have the well-known protecting effect of the finite-time measurement. On the other hand, the measurement apparatus has its already-observed effect of increasing the reduction rate of the coherences.

The coherence has its rate of decay sharpened as the environment temperature rises. From the graphs, we can also see that as the environmental temperature rises the population has its decrease rate attenuated, *i.e.*, for a higher temperature, we have a lower measurement error. Hence we see that the environment can have contradictory effects over the measuring process: the coupling intensity η acts to increase the error associated to the measurement process and decrease the measurement time; however, the temperature T acts to reinforce the effects of the system-measurement apparatus coupling λ , preventing the decay and increasing the measurement time.

This curious effect is a fortuitous coincidence caused by our choice of ω_0 and initial state. With $\omega_0 = 0$, the thermal energy from the environment will eventually lead to a state of thermal equilibrium between the two systems that will stabilize both populations at the same value. Starting at $\rho_{11}(0) = 0.5$, our initial state is already the expected final state. An increase in temperature, in this case, only makes faster the approach of the equilibrium situation.

The maintenance of the system in the excited state, however, can be verified even with the ω_0 and T parameters above zero. As illustrated in fig. 8, we can, with a strong enough choice of the measurement coupling λ , keep an ensemble of initially excited systems as close as possible to their original states even at times when they would normally have completely decayed by themselves. This is not simply a more efficient way of performing a measurement of their initial state, but may be a means of observing the quantum Zeno effect [33] (*i.e.*, keeping a system in its excited state by observing it) for finite-time measurements.

Finally, fig. 9 shows curves for non-zero environmental temperature, considering constant system-environment coupling and changing the frequency of system and its coupling with the measurement apparatus. We see that the introduction of ω_0 does not change the evolution of the moduli of the coherences, but intensifies the population decrease for a fixed λ .

Contrary to the case with phase-damping interaction, here we verified some curious effects when we change the system-environment interaction to amplitude damping:

- both system-measurement apparatus coupling λ and environment temperature T can have the effect of preserving the system in the excited state; the first effect is universal, while the second only occurs for certain values of the initial population and temperature, and is a direct consequence of the repopulation of the excited state caused by the thermal energy of the environment;
- both the system frequency ω_0 and the system-environment coupling η intensify the decrease of the population;
- in general, the conclusions obtained by the measurement of the x -component with phase-damping interaction are valid in the present case, except, perhaps, the formula for the upper limit of the measurement duration.

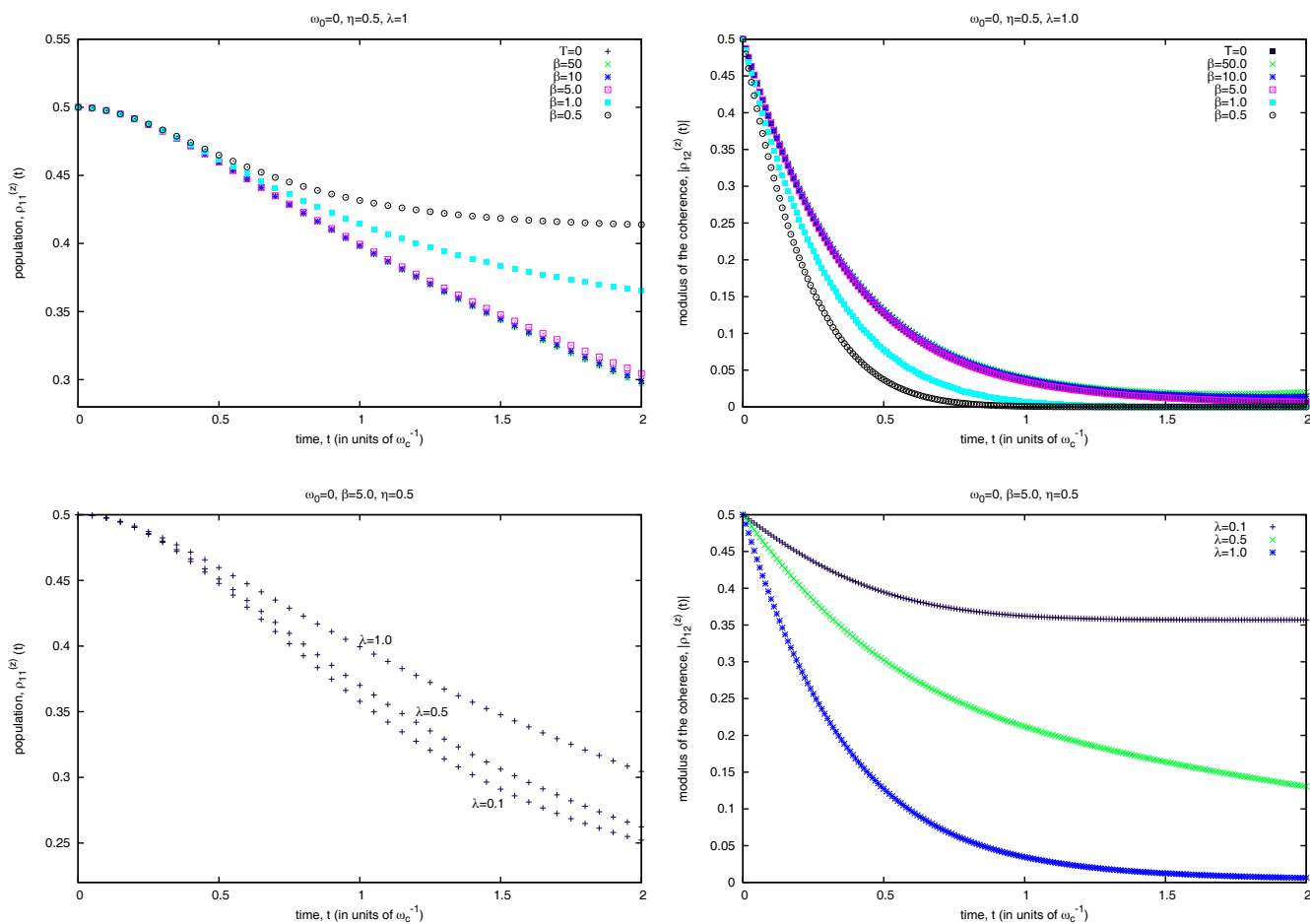


Fig. 7. Introduction of temperature of the environment for the amplitude-damping interaction.

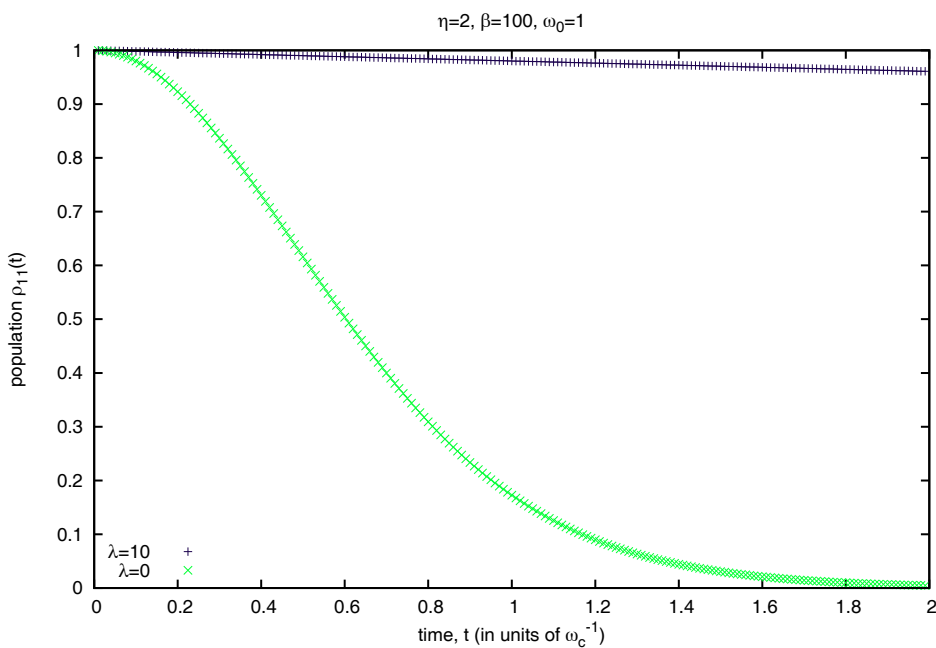


Fig. 8. Attenuated decay caused by the finite-time measurement of the excited state of the system. In green, the curve corresponding to the free evolution of the population; in red, the one indicating its evolution during measurement.

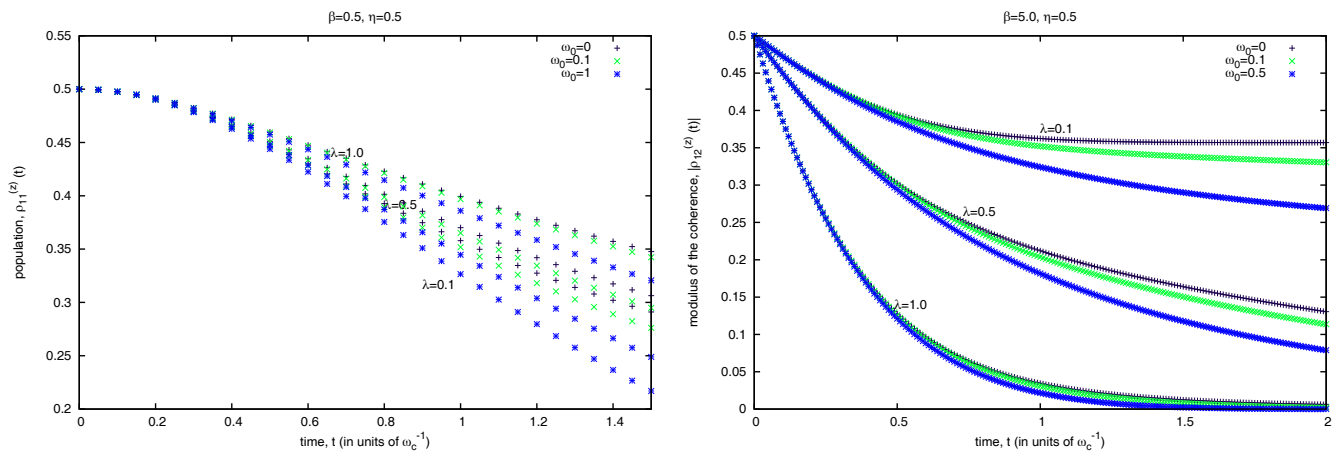


Fig. 9. Populations and moduli of the coherences, and their dependence on λ and T .

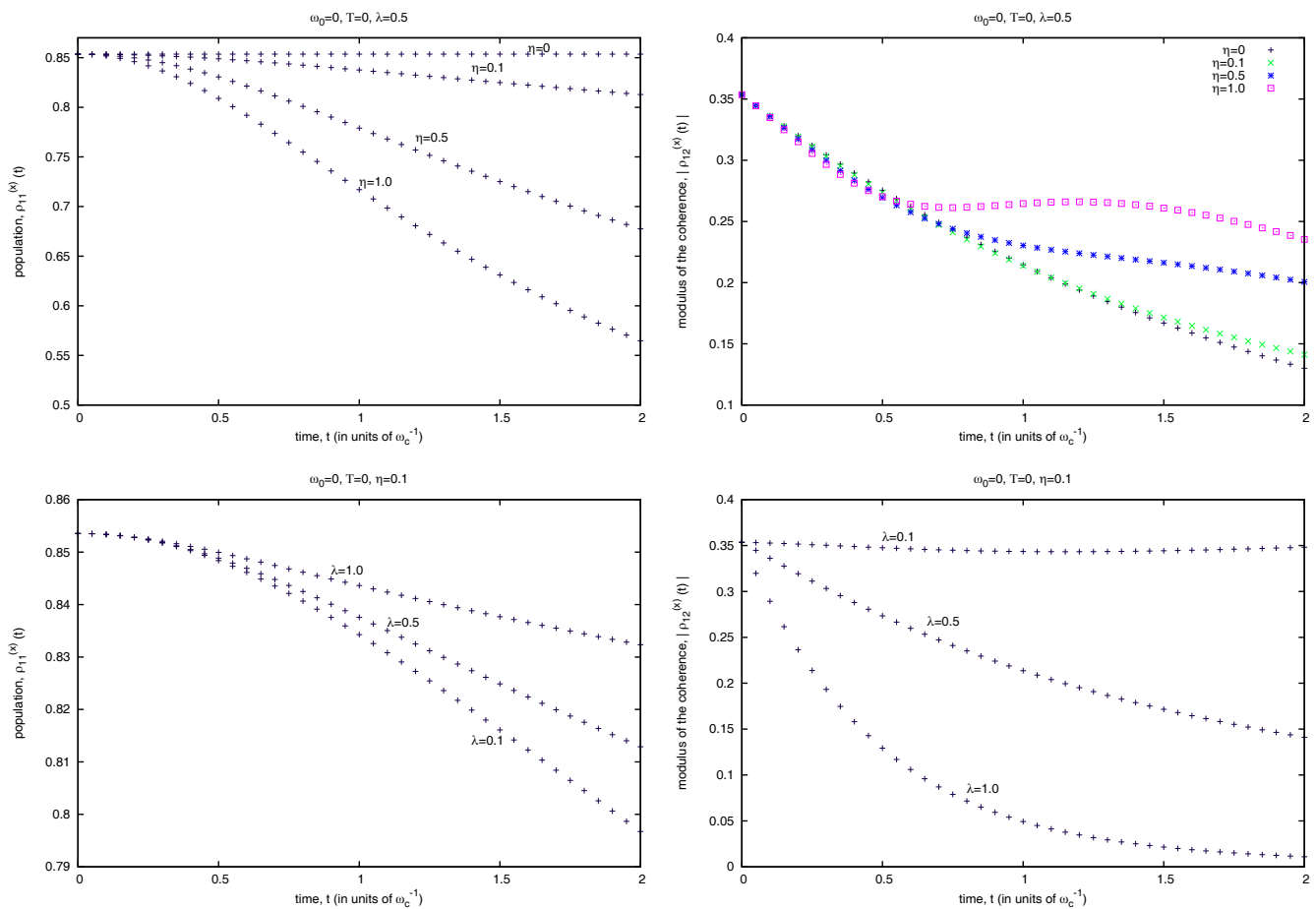


Fig. 10. Populations and coherences for two values of λ and different values of η .

5.2.2 The x -component measurement

Figure 10 shows population and coherence curves for several values of λ and η , while keeping $\omega_0 = T = 0$. As previously observed, the system-environment interaction acts in the sense of accentuating the population decrease and, consequently, the error associated to the measurement process. However, the measurement apparatus still keeps the populations close to their original values.

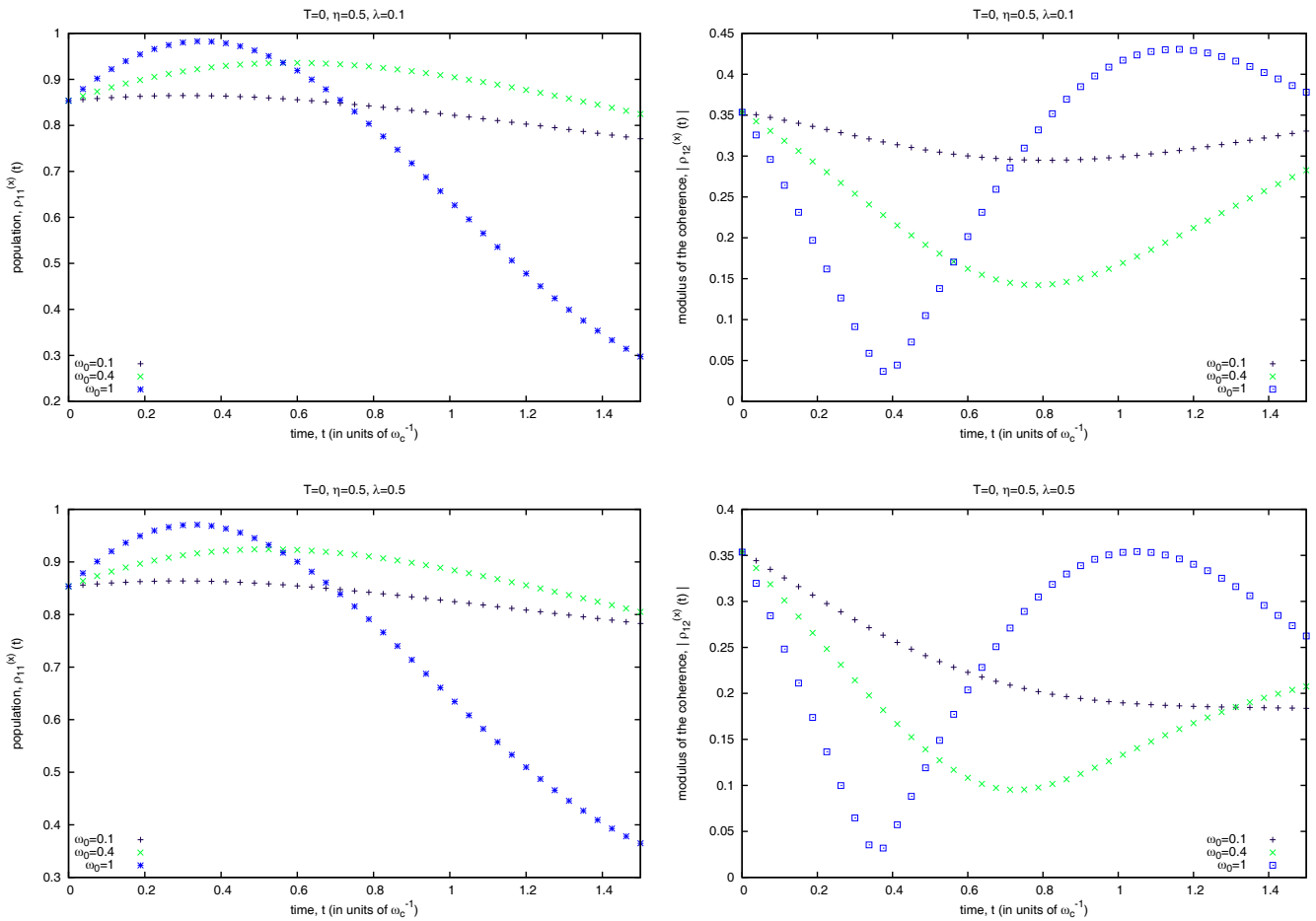


Fig. 11. Populations and coherences obtained for a fixed η , varying λ and ω_0 .

Although we cannot, in this case, obtain a simple expression for the duration of the measurement, we still use the coherences to establish the time at which the system-environment interaction can be interrupted and the reading of the state accomplished—in this case, the time when the coherences assume the constant asymptotic value. Obviously, in more general cases, when the behavior of the system is not simple (the coherences no longer display a monotonic decrease), its physical properties must be considered to the establishment of the measurement time. In these non-monotonous cases, there are at least two possible criteria that could be taken to determine the end of the measurement: the instant when the moduli of the coherences reach zero, or when they assume an asymptotically constant value.

The next step is to introduce a system frequency ω_0 . In this case, we observe a similarity with the behavior of the measurement of the x -component for phase-damping interaction: the populations do not exhibit monotonic behavior anymore, instead displaying a maximum point. As the system-environment coupling increases, both its intensity and the time when it occurs decrease. On the other hand, increasing the system-measurement apparatus coupling diminishes the maximum intensity.

Figure 11 shows that the element that determines the qualitative format of the curves is the frequency of the system ω_0 . One should note, while observing these results, that all of them were plotted in the basis of the measurement, that is, $\hat{\sigma}_x$. These populations depend on the real part of the coherences in the basis of $\hat{\sigma}_z$, which is expected to oscillate when $\omega_0 \neq 0$. For example, in the case of a spin in a z -oriented field, the expectation values of $\hat{\sigma}_x$ and $\hat{\sigma}_y$ change while the spin rotates around the z -axis. This explains the non-monotonous behavior of the populations, a phenomenon observed previously in fig. 2(a).

Lastly, we analyse the effects of the environmental temperature. For the present case, contrary to the previous section, we verified that, for a larger environmental temperature, the rate of change of the populations is increased. Then, the environment—through T —acts to increase the measurement error, reinforcing the fact that the temperature-originated protection found in the previous section was merely fortuitous.

Figure 12 shows several curves for different environment temperatures and $\omega_0 = 0$ and, after that, curves where all relevant parameters are present. Once again, the qualitative behavior is determined by ω_0 .

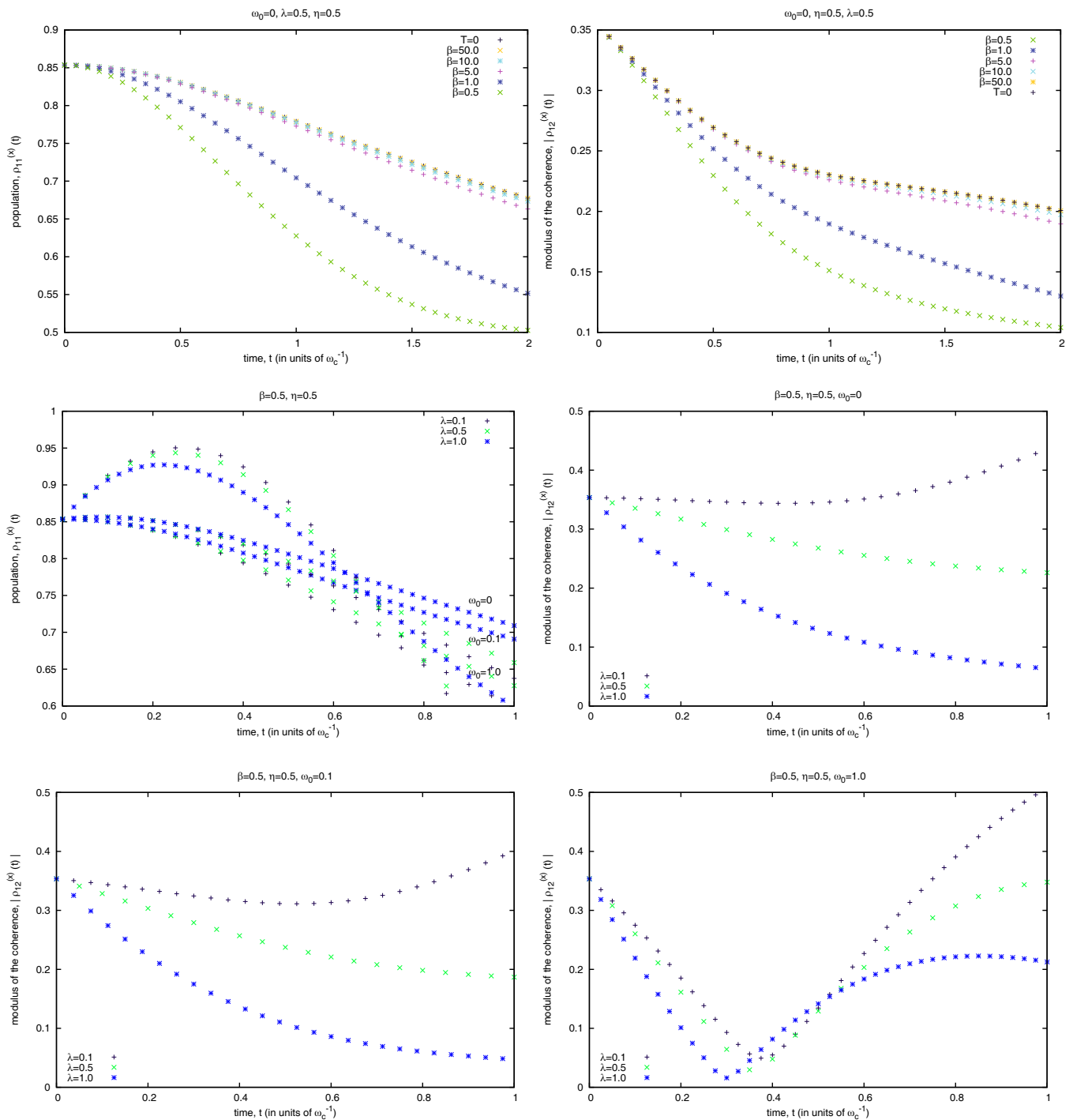


Fig. 12. Effect of the introduction of T , followed by the introduction of T and ω_0 . The last three graphs contain the coherences corresponding to the populations plotted in the third one. To avoid confusion caused by the superposition of different curves, they were broken in three.

6 Conclusions and perspectives

In this work, we employed the formalism that we developed to treat the hybrid formulation of the master equation [18], which helped us to simplify the analytic solution, although the system of equations encountered still had to be solved numerically. In both cases, phase and amplitude damping, the interaction between the system and the measurement apparatus diminishes the effects of the noise on the population of the main system, allowing us to generalize our previous conclusions in this sense [26]. This means that in both cases we are capable of performing a measurement

more efficiently if instead of measuring it instantly at $t > 0$, we perform a finite-time measurement from 0 to t , even at finite temperature. Likewise, for finite-time measurements, an increase in the system-apparatus coupling constant λ is capable of making their results more reliable.

The possibility of application of this kind of measurement to improve the quality of the results depends, however, on the practical existence of measurements that can be performed for a finite period of time, in accordance to the model. In the following appendix, we propose a verification of our hypothesis by a simple experimental setting that, if yielding positive results, would not only affect fundamental aspects of quantum theory but, also, other areas such as quantum information theory [34].

Besides the assumption that measurements are finite in time, we took the additional step of approximating the system-apparatus interaction as a Markovian process. Even though having the advantage of simplifying our calculations, this is a hypothesis far less straightforward to justify than the finite-time measurement. Future prospects of our research include eliminating this approximation by letting the λ^2 vary in time [35] and seeing the effects of this in the noisy measurement process.

CAB acknowledges support from Coordenação de Aperfeiçoamento de Pessoal de Nível Superior (CAPES) and Fundação de Amparo à Pesquisa do Estado de São Paulo (FAPESP), project number 2011/19848-4, Brazil, and to A.O. Caldeira for hospitality and useful discussions. LAdC acknowledges support from CAPES. RdJN acknowledges support from Conselho Nacional de Desenvolvimento Científico e Tecnológico (CNPq), Brazil.

Appendix A. Proposed experimental test

Beyond what has been shown in [28], here we propose an alternative experimental application of our formalism. Throughout this and previous articles, we made the bold assumption that the measurement can ultimately be described as a finite-time interaction between the system and a large number of (traced-out) degrees of freedom of the apparatus. Moreover, we assumed that this interaction could be described as Markovian. The accuracy of these assumptions is far from uncontroversial, but could be verified in the experimental test described below, which is based on the theory of weak measurements [36]. We should note, before proceeding, that in this test we are mostly interested in the validity of the first assumption, that is, the possibility of making finite-time measurements in practice. In case the Markovian approximation is not valid the experiment can still be used to test the extension of our model to non-Markovian measurement apparatus, currently a work in progress.

In this experimental setting, we analyse what happens when we measure the magnetic moment of a spin-1/2 particle with two Stern-Gerlach apparatus, which corresponds to the kind of two-state measurement described in the body of this article. The first apparatus performs a “weak” measurement, *i.e.*, one that does not completely destroy the coherences; and the second promoting the full collapse of the wave function. As the second equipment’s task is simply to measure the state of the spins of the particle after they have been through the first equipment, we shall not concern ourselves with its inner workings, and it will not be necessary for this second apparatus to actually be a Stern-Gerlach.

We choose the direction of the z axis so the final measurement is done along it. As this experiment will yield trivial results if we choose the observable measured by the weak measurement as the same the second one, we will tilt the first apparatus with an angle β in respect with the z axis. In this case, the observable being measured by it will be:

$$\hat{\sigma}_\beta = \cos \beta \hat{\sigma}_z + \sin \beta \hat{\sigma}_x,$$

where we are calling the direction along which the particles move the y axis.

We shall not make any assumptions about the initial state of the spins of the particles, allowing it to be represented by any 2×2 density matrix $\hat{\rho}(0)$. When these particles cross the first equipment, which we will consider noiseless for simplicity, it will reduce their coherences (in the basis of eigenstates of $\hat{\sigma}_\beta$) to a fraction $0 < b < 1$ of their original value, while leaving the populations intact. For “strong”, or “complete” measurements, the wave function collapse would result in the coherences completely vanishing ($b = 0$), but for a weak measurement b is actually closer to one.

Explicitly, we can write that, if a particle enters the apparatus at $t = 0$ and leaves it at τ , its final state will be:

$$\hat{\rho}(\tau) = \frac{1}{2} [1 + b(\tau)] \hat{\rho}(0) + \frac{1}{2} [1 - b(\tau)] \hat{\sigma}_\beta \hat{\rho}(0) \hat{\sigma}_\beta.$$

In the equation above, we have given the fraction b a time dependence, which is precisely the hypothesis we wish to test. If the measurement is instantaneous, this function will be constant, while it will display other kinds of behavior if it is actually a dynamical process. Therefore, our experiment should be capable of providing us information about the form of $b(t)$.

The final measurement, if performed correctly, will give us simply the expectation value of the variable $\hat{\sigma}_z$ at $t = \tau$, regardless of how much time it takes to extract this information from the quantum system, or of how this process is performed. Therefore, from the equation above, we can conclude that the expectancy value of the experiment will be:

$$\langle \hat{\sigma}_z \rangle(\tau) = [\cos^2 \beta + b(\tau) \sin^2 \beta] \langle \hat{\sigma}_z \rangle(0) + \frac{1}{2} [1 - b(\tau)] \sin(2\beta) \langle \hat{\sigma}_x \rangle(0),$$

if we consider that the system does not evolve between the two measurements, *i.e.* $\omega_0 = 0$.

Comparing this theoretical formula with the results of the experiments described below, one would be able to deduce the form of the function $b(t)$. Indeed, the results of $\langle \hat{\sigma}_z \rangle(\tau)$ and $\langle \hat{\sigma}_z \rangle(0)$ can be measured directly by turning on or off the first Stern-Gerlach apparatus. If $\langle \hat{\sigma}_x \rangle(0)$ cannot be known from the preparation of the spins, we can eliminate it from the equation by taking $\beta = \pi/2$:

$$\langle \hat{\sigma}_z \rangle(\tau) = b(\tau) \langle \hat{\sigma}_z \rangle(0), \quad \beta = \frac{\pi}{2}.$$

This is probably the preferred setting of the experiment, but we will proceed nevertheless treating β as any angle, to keep our results as general as possible. The only thing we have to keep in mind is that we cannot choose $\beta = n\pi$, $n \in \mathbb{Z}$, as this would reduce the expression above to something trivial.

Appendix A.1. Checking if the measurement is “weak”

The experiment proposed requires the assumption that the first measurement is weak. If it turns out that the first Stern-Gerlach is actually completely collapsing the wave function, there will be no meaningful results.

In this undesirable situation, we would have $b = 0$, yielding a measurement of:

$$\langle \hat{\sigma}_z \rangle_{b=0}(\tau) = \cos^2 \beta \langle \hat{\sigma}_z \rangle(0) + \frac{1}{2} \sin(2\beta) \langle \hat{\sigma}_x \rangle(0).$$

We should, therefore, make sure our test results are sufficiently distant from those expected when the measurement is not weak. The difference between the preferred and failed cases is of:

$$\Delta_z \equiv |\langle \hat{\sigma}_z \rangle_{b \approx 1}(\tau) - \langle \hat{\sigma}_z \rangle_{b=0}(\tau)| \approx \left| \cos^2 \beta \langle \hat{\sigma}_z \rangle(0) - \frac{1}{2} \sin(2\beta) \langle \hat{\sigma}_x \rangle(0) \right|.$$

Therefore, it is desirable to choose the initial conditions and the angle β so that Δ_z is bigger than our experimental errors, in order to distinguish the case when the measurement is weak from the case when it is too strong.

In the best setting, where $\beta = \pi/2$, the undesirable situation has $\langle \hat{\sigma}_z \rangle_{b=0}(\tau) = 0$. This means that, as long as we choose an initial condition satisfying $|\langle \hat{\sigma}_z \rangle(0)| > 0$, we just have to measure an average value distinguishable from zero to be sure we are indeed performing “weak” measurements. The error of the experiment, therefore, must be kept below $\Delta_z = |\langle \hat{\sigma}_z \rangle(0)| > 0$. On the other hand, it may also be important to verify if $\langle \hat{\sigma}_z \rangle(\tau)$ is distinguishable from $\langle \hat{\sigma}_z \rangle(0)$, *i.e.*, that **some** intermediary measurement is being performed.

Appendix A.2. Varying times of measurement

The previous experiment can be only used to make sure that there is a b function in action, but gives no information about the time dependency of that function. To acquire information about it, we must vary the measurement periods τ and see what effect these have in the final result. There are two possible ways of varying the time of exposure in a Stern-Gerlach equipment: you can change the velocity with which the particles cross the apparatus, or you can change the length of their path. It is just important not to change the strength of measurement (by altering the gradient of the magnetic field, for example), instead of the time of exposure of the spin.

In its most general form, the average value measured will be:

$$\langle \hat{\sigma}_z \rangle(\tau) = A + b(\tau)C,$$

where A, C are constants. Once we calculate them using the known values of the initial conditions and the tilting of the intermediary measurement β , we can plot the values of $b(\tau)$, thereby verifying whether it is constant or if measurement indeed has a time dependency. For the situation where $\beta = \pi/2$, the function becomes simply a renormalization of the measured average values:

$$b(\tau) = \frac{\langle \hat{\sigma}_z \rangle(\tau)}{\langle \hat{\sigma}_z \rangle(0)}.$$

If the measurement is an instantaneous phenomenon that does not depend on the time of interaction of the apparatus, we should encounter a constant, while a smooth dynamical measurement would produce a positive function with the limits $b(\tau \rightarrow 0) = 1$, $b(\tau \rightarrow \infty) = 0$.

Appendix A.3. Connection with our model of measurement

In our model of measurement as a Markovian interaction between the system and the measurement apparatus, the $b(\tau)$ function has the form of a negative exponential:

$$b(\tau) = e^{-2\lambda^2\tau},$$

where λ is the constant that represents the strength of the coupling between the system and the measurement apparatus. This is a function that satisfies the limits given in the previous section, thus being a plausible candidate for the results that can be found experimentally.

If controlling the time the particles remain under measurement is not a feasible task in some laboratory, one could vary instead the coupling strength with the measurement apparatus (represented by the rate of change of the magnetic field, in the case of the Stern-Gerlach experiment). If the dependence found between b and λ^2 in this case is exponential, it will not be a confirmation that measurement is a finite-time phenomenon, but it could be a good first step towards confirming our theory. Conversely, if we are capable of controlling τ and measuring b with good precision, we can use the equation above to calculate λ^2 , transforming this theoretical parameter into something concrete.

We should note, finally, that the heart of the Markovian approximation is that λ^2 is a positive constant. In case it is not, we would still find some change in the value of $b(t)$, even though not as simple as a negative exponential. Therefore, this experiment could still be used to determine the finite-time length of the measurement, while our model would have to be altered to account for varying of λ^2 . As mentioned in the final section of this article, these adaptations are currently work in progress.

References

1. M. Jammer, *The Philosophy of Quantum Mechanics: The Interpretations of Quantum Mechanics in Historical Perspective* (Wiley, New York, 1974).
2. J.A. Wheeler, W.H. Zurek, *Quantum Theory and Measurement* (Princeton University Press, Princeton, 1983).
3. B.L. van der Waerden, *Sources of Quantum Mechanics* (North Holland Pub. Co., Amsterdam, 1967).
4. G.S. Im, Arch. Hist. Exact Sci. **50**, 73 (1995).
5. P.A.M. Dirac, Proc. R. Soc. London Sect. A **112**, 661 (1926).
6. K. Gottfried, Am. J. Phys. **79**, 261 (2011).
7. J. von Neumann, *Mathematical Foundations of Quantum Mechanics* (Princeton University Press, Princeton, 1953).
8. H. Everett III, Rev. Mod. Phys. **29**, 454 (1957).
9. J.A. Wheeler, Rev. Mod. Phys. **29**, 463 (1957).
10. B.S. Dewitt, N. Graham, *The Many-Worlds Interpretation of Quantum Mechanics: A Fundamental Exposition by Hugh Everett, III* (Princeton University Press, Princeton, 1973).
11. F. Freitas, O. Freire Jr., Rev. Bras. Ensino Fís. **30**, 2307 (2008) (open access).
12. A. Peres, Phys. Rev. A **61**, 022116 (2000).
13. G. Lindblad, Commun. Math. Phys. **48**, 119 (1976).
14. H.-P. Breuer, F. Petruccione, *The Theory of Open Quantum Systems* (Oxford University Press, Oxford, 2002).
15. C.A. Brasil, F.F. Fanchini, R.d.J. Napolitano, Rev. Bras. Ensino Fís. **35**, 1303 (2013) (open access).
16. I. Percival, *Quantum State Diffusion* (Cambridge University Press, Cambridge, 1998).
17. J.D. Crasser, S.M. Barnett, J. Jeffers, D.T. Pegg, Opt. Commun. **264**, 352 (2006).
18. C.A. Brasil, R.d.J. Napolitano, Eur. Phys. J. Plus **126**, 91 (2011).
19. S. Nakajima, Prog. Theor. Phys. **20**, 948 (1958).
20. R. Zwanzig, J. Chem. Phys. **33**, 1338 (1960).
21. L.S. Schulman, Phys. Rev. A **57**, 1509 (1998).
22. P. Facchi, S. Pascazio, Fortschr. Phys. **49**, 941 (2001).
23. K. Jacobs, D.A. Steck, Contemp. Phys. **47**, 279 (2006).
24. A. Barchielli, L. Lanz, G.M. Prospero, Nuovo Cimento B **72**, 79 (1982).
25. M. Caves, G.J. Milburn, Phys. Rev. A **36**, 5543 (1987).
26. C.A. Brasil, L.A. de Castro, R.d.J. Napolitano, Phys. Rev. A **84**, 022112 (2011).
27. C.A. Brasil, L.A. de Castro, R.d.J. Napolitano, Found. Phys. **43**, 642 (2013).
28. Y. Yan, J. Zou, B.-M. Xu, J.-G. Li, B. Shao, Phys. Rev. A **88**, 032320 (2013).
29. H.M. Wiseman, G.J. Milburn, Phys. Rev. Lett. **70**, 548 (1993).
30. H.M. Wiseman, Phys. Rev. A **49**, 2133 (1994).
31. J.H. Reina, L. Quiroga, N.F. Johnson, Phys. Rev. A **65**, 032326 (2002).
32. A.I. Lvovsky, B.C. Sanders, W. Tittel, Nature Photon. **3**, 706 (2009).
33. B. Misra, E.C.G. Sudarshan, J. Math. Phys. **18**, 756 (1977).
34. M.A. Nielsen, I.L. Chuang, *Quantum Computation and Quantum Information* (Cambridge University Press, Cambridge, 2000).
35. J. Piilo *et al.*, Phys. Rev. A. **79**, 062112 (2009).
36. Y. Aharonov, D.Z. Albert, L. Vaidman, Phys. Rev. Lett. **60**, 1351 (1988).